POLITECNICO DI MILANO

Scuola di Ingegneria Industriale e dell'Informazione

Corso di Laurea Magistrale in Ingegneria Elettrica

RESEARCH AND DESIGN ON 1KW HIGH POWER DENSITY LLC RESONANT CONVERTER BASED ON GAN DEVICE

Relatore: Prof. Enrico Ragaini

Tesi di Laurea Magistrale di:
Yazhen Ji
Matr. 854630

Anno Accademico 2017-2018

CONTENTS

CONTENTS 1

LIST OF FIGURES 3

LIST OF TABLES 6

SOMMARIO 7

ABSTRACT 8

1 INTRODUCTION 9

1.1 Background of research 9

1.2 Design requirement 19

2 THE ANALYSIS OF LLC RESONANT CONVERTER 20

2.1 Analysis of the working process of LLC resonant converter 20

2.2 Modeling of LLC resonant converter and DC gain characteristics analysis 28

2.3 Summary 33

3 CONVERTER DESIGN 34

3.1 Design of main circuit parameters 34

3.1.1 Design of magnetizing inductor 35

3.1.2 Design of resonant inductor 37

3.1.3 Design of resonant capacitor 37

3.2 Device selection 37

3.2.1 Selection of primary side device 38

3.2.2 Selection of secondary side device 42

3.3 Main circuit simulation 45

3.4 Integrated and thermal design of converter 47
3.4.1 Traditional structure design 48
3.4.2 Optimized structure design 50
3.4.3 Thermal simulation of converter 51
3.5 Design of control and drive circuit 53
3.5.1 Design of control circuit 53
3.5.2 Selection and optimization of isolation and drive chip 55
3.5.3 Layout optimization of PCB 56
4 EXPERIMENT AND RESULT ANALYSIS 59
4.1 Experimental platform and prototype 59
4.2 Experimental results and analysis 61
4.3 Summary 65
5 CONCLUSION AND PROSPECT 66
6 REFERENCES 69

LIST OF FIGURES

Figure 1-1 The high power density power supply 9

Figure 1-2 The techniques in design 10

Figure 1-3 Full-bridge phase-shifted diagram 11

Figure 1-4 Structure of resonant converter network 12

Figure 1-5 Diagrams of equivalent circuit 13

Figure 1-6 Planar transformer 16

Figure 1-7 Diagram of synchronous rectification 17

Figure 1-8 Converters produced by SynQor 18

Figure 1-9 Converters produced by Vicor company 18

Figure 2-1 Diagram of LLC half-bridge converter 21

Figure 2-2 Diagram of LLC converter when $f_s = f_{r1}$ 22

Figure 2-3 Diagrams of switching process 25

Figure 2-4 Diagram of LLC converter when $f_{r2} < f_s < f_{r1}$ 26

Figure 2-5 Diagram of current in $[t_{10} \sim t_2]$ 27

Figure 2-6 Diagram of LLC converter when $f_s > f_{r1}$ 27

Figure 2-7 Diagram of current in $[t_1 \sim t_{20}]$ 28

Figure 2-8 Topology and models of LLC resonant converter 29

Figure 2-9 Gain curve of LLC resonant converter (L_n=5) 31

Figure 2-10 Gain curve of LLC resonant converter (L_n=15) 32

Figure 3-1 Topology of the converter 34

Figure 3-2 GS66508T capacitance characteristics 36

Figure 3-3 Voltage and current waveform of GaN when turned off 40

Figure 3-4 Relationship between $R_{DS(ON)}$ of GS66508T and temperature 41

Figure 3-5 Diagram of synchronous rectifying waveform in secondary side 43

Figure 3-6 Relationship between $R_{DS(ON)}$ of EPC2032 and temperature 44

Figure 3-7 Circuit simulation model of LLC resonant converter 46

Figure 3-8 LLC main circuit simulation waveform 47

Figure 3-9 Diagram of traditional structure with FR4.. 48

Figure 3-10 Diagram of the MCPCB 49

Figure 3-11 Diagram of DBC structure 49

Figure 3-12 650V/150A half bridge power module of GaN device 50

Figure 3-13 600V/30mΩ half bridge power module of GaN device 50

Figure 3-14 Diagram of optimized structure 51

Figure 3-15 Simulation model diagram of heat dissipation 52

Figure 3-16 Simulation results of heat dissipation scheme 52

Figure 3-17 Diagram of control and drive circuit... 53

Figure 3-18 Package and pin diagram of STM8S003F3P6 55

Figure 3-19 Pin diagram of Si8271 56

Figure 3-20 Diagram of driving resistance optimization... 56

Figure 3-21 Diagram of PCB wiring 58

Figure 4-1 Platform for the experiment 59

Figure 4-2 Prototype for the experiment 60

Figure 4-3 Waveform of PWM 62

Figure 4-4 Driving waveform.. 62

Figure 4-5 Waveform of V_m and V_{gs_S2} 63

Figure 4-6 Experimental waveform diagram.. 64

Figure 4-7 Temperature distribution diagram on the front of the converter 64

Figure 4-8 Experimental efficiency curve of prototype 65

LIST OF TABLES

Table 1-1 Material properties of silicon, silicon carbide and gallium nitride 14

Table 1-2 Main parameter of high power density converters... 18

Table 1-3 Design paramters... 19

Table 3-1 Parameters of the converter... 34

Table 3-2 Parameters of GS66508T 39

Table 3-3 Parameters of 100V GaN devices 42

Table 3-4 Comparison of various substrate parameters 49

Table 4-1 Name and function of the instrument... 59

Table 4-2 Device selection and parameter of prototype... 60

SOMMARIO

Con lo sviluppo dell'economia e dell'industria, nel mondo, la domanda e l'obbligo di approvvigionamento di energia è in costante aumento nel settore della difesa nazionale, nuove forme di energia, i veicoli elettrici e di comunicazione. La comunicazione e la forte densità di potenza sono l'obiettivo dello sviluppo dell'alimentatore. Attraverso il confronto e l' analisi, LLC convertitore può raggiungere morbido passaggio risonanza in tutto il carico, ridurre la perdita e l'elevata efficienza di passaggio, ed è stato ampiamente interessato al potere la tipologia del campo. Come un dispositivo di potenza emergente negli ultimi anni, Gan è dei dispositivi più veloci di commutazione e la perdita di stato inferiore e dispositivi. L 'uso di GaN dispositivi è favorevole ad ulteriori miglioramento dell'efficienza e la densità di potenza dei convertitori di energia. Il dispositivo è diventato un hotspot - ricerca nel campo dell'energia. L'applicazione di GaN alla LLC risonante convertitore può migliorare ulteriormente la densità di potenza, di efficienza e di altri parametri di rendimento del convertitore. Ma al momento, ci sono pochi studi correlati in patria e all'estero.

Il documento introduce il funzionamento dello stato e il passaggio alle caratteristiche del convertitore LLC risonante. In questo documento, il guadagno delle caratteristiche sono analizzati e sintetizzati sulla base di un'analisi basilare e matlab software. L'appropriato stato LLC risonante convertitore è stabilita. La selezione e l'analisi dell'interruttore, è fatta. I principali parametri del convertitore di risonanza sono progettati, calcolati e simulati. Molti comuni strutture e una struttura ottimale dissipazione di calore rispetto flotherm (termica basata sul software di simulazione). I dettagli di progettazione del convertitore, come l'influenza di guidare i segnali in GaN dispositivi di isolamento, chip, guido chip selezione, il pcb fili e altre questioni sono ulteriormente elaborati e ottimizzati.

Infine, la progettazione del prototipo sperimentale e l'efficienza della curva del prototipo viene dato. Dai dati sperimentali mostrando che la soft switch è finita nel convertitore - tubo. La tensione d'ingresso è 270V. L 'output di tensione è stabile a 28V, che si riunisce il progetto target. Il potere è 1kw. L'efficienza del prototipo è superiore al 93%, di cui la massima efficienza è 97.6%. La progettazione e ottimizzazione per l'alta densità di potenza sonora sulla base di GaN dispositivo convertitore LLC è verificata dall'esperimento.

ABSTRACT

With the development of economy and industry in the world, the demand and requirement of power supply is increasing continuously in the fields of national defense, new energy, electric vehicle and communication. The high-efficiency and high power density is the development goal of power supply. By comparing and analyzing, LLC resonant converter can achieve soft switching in all load, reduce switching loss and high efficiency of switch, and has been widely concerned in power topology field. As an emerging power device in recent years, GaN devices have higher switching speed and lower state loss than Si devices. The use of GaN devices is conducive to further improving the efficiency and power density of power converters. The GaN device has become a research hotspot in the field of power supply. The application of GaN to the LLC resonant converter can further improve the power density, efficiency and other performance parameters of the converter.

The paper introduces the working state and the switching characteristics of LLC resonant converter. In this paper, the gain characteristics are analyzed and summarized based on fundamental analysis and MATLAB software. The suitable working state of LLC resonant converter is established. The selection and analysis of the switch tube is made. The main parameters of the resonant converter are designed, calculated and simulated. The main loss of the circuit is calculated. The structure of the converter is designed and an optimized structure scheme is put forward. Several common heat dissipation structures and an optimized structure are compared based on the FloTHERM (thermal simulation software). The details of designing the converter, such as the influence of drive signals on GaN devices, controller, isolation chip, drive chip selection, PCB wiring and other issues are further elaborated and optimized.

Finally, the design of the experimental prototype and the efficiency curve of the prototype are given. The experimental results show that the soft switch is finished in the converter switch tube. The input voltage is 270V. The output voltage is stable at 28V, which meets the design target. The power is 1kW. The efficiency of the prototype is above 93%, which the peak efficiency is 97.6%. The design and optimization on the high power density LLC resonant converter based on GaN device are verified by experiment.

1 INTRODUCTION

1.1 Background of research

In recent years, with the rapid development of the second industry, which is mainly based on manufacturing industry, the demand for power supply, in the new energy field, the recent rapid developing the electric vehicle and the communication field, is increasing. It provides great opportunities for power electronics and power design industry, and also poses corresponding challenges to power technology. Among them, DC/DC switching power supply with high efficiency and high power density has become an important choice for the design of power supply.

Figure 1-1 The high power density power supply

With the development of power supply, various technologies and applications have sprung up. The proposal and application of soft switching technology, new wide band gap semiconductor device, planar transformer and synchronous rectifier technology provide the possibility to achieve high efficiency and high power density [1].

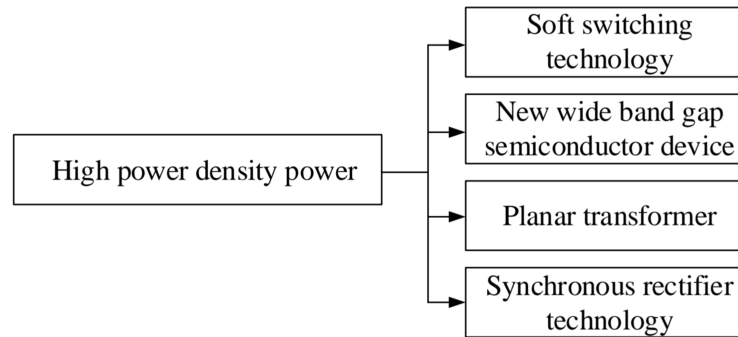

Figure 1-2 The techniques in design

Increasing the working frequency of the switching power supply can effectively reduce the volume of the transformer, especially the transformer. It is a direct way to improve the power density of the power supply module. But increasing the working frequency of the switching power supply will also increase the switching loss of the switch device, which makes the efficiency of the converter lower, the heat dissipation pressure of the switch device increases, and even the serious electromagnetic interference is introduced [2]. In order to avoid the effect of switching losses under high working frequency, soft switching technology is proposed accordingly and has been widely applied in high power density supply. At present, there are resonant network topology and soft switching topology controlled by PWM. The soft switch topology controlled by PWM is represented by full-bridge phase-shifted circuit [3]. Figure 1-3 is a full-bridge phase-shifted topology diagram and control waveform diagram.

The difference between the full-bridge phase-shifted PWM control and the traditional full bridge control mode lies in the driving phase of the diagonal switch tubes (such as Q1 and Q3, Q2 and Q4) [4]. The phase difference is formed to realize the adjustment of voltage and the realization of soft switching. However, when the full-bridge phase-shifted control mode is carried out under no load or light load, the energy of soft switching with the lag phase comes from leakage inductance. If leakage energy is insufficient, zero voltage switching will be difficult to achieve [5]. The full-bridge phase-shifted circuit also has the problem of loss of duty cycle.

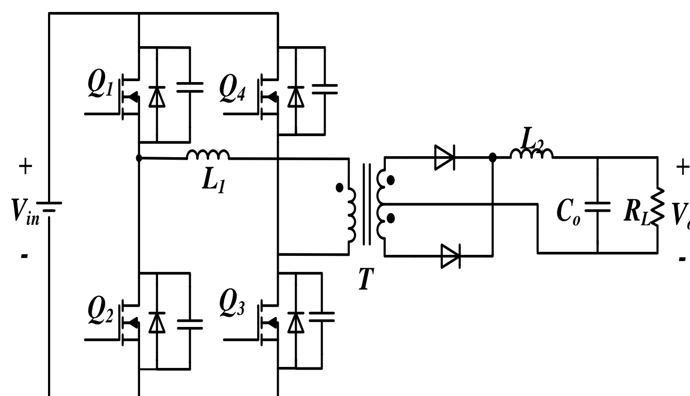

（a）Full-bridge phase-shifted circuit

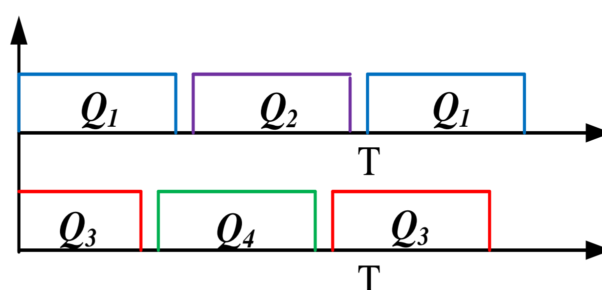

（b）Diagram of control waveform

Figure 1-3 Full-bridge phase-shifted diagram

The main way to achieve soft switching by using resonant converter network is to add resonant devices such as capacitors and inductors in the converter. By doing so, the soft switching of power devices can be realized. The structure of the resonant network converter is shown in Figure 1-4. In the resonant converter, because the current waveform in the loop is close to the sine wave, it has certain advantages in the subsequent electromagnetic compatibility design of the converter [6]. The full-bridge phase-shifted adjusts the voltage by controlling the phase and duty time. The resonant converter mainly adjusts and controls the output voltage by adjusting the working frequency, so the drive duty ratio of the switch tube is fixed and the utilization rate is high. At present, the common resonant converters are divided into parallel resonant converter (PRC), series resonant converter (SRC) and series parallel resonant converter including LLC and LCC [7]. The equivalent circuit diagram of all types of resonant converters is shown in Figure 1-5.

For the series resonant converter, the DC voltage gain of a series resonant converter can not exceed 1 due to the load and the resonant network. In light load, the load impedance is much

larger than that of the resonant network. If you want to adjust the output voltage, a very high working frequency is needed. In order to control the output voltage, the working frequency needs to be close to infinity. For parallel resonant converters, it is inevitable that a high current is needed because the resonant network and the load are connected in parallel. This increases the difficulty in the application of high power density or load changing applications. Series parallel resonators combine the advantages of series resonant converter and parallel resonant converter to solve their problems to a certain extent. Series parallel resonant converter is divided into LCC resonant converter and LLC resonant converter. The LCC resonant converter contains two resonant capacitors. But in general converters, the capacitance is relatively small and the cost is high. And for the isolated DC/DC converter, the LCC resonant converter does not make use of the transformer leakage inductance [8]. But the LLC resonant converter can use two inductors to use the corresponding relationship between the transformer leakage inductance and the excitation inductor respectively, which is beneficial to the realization of magnetic integration, and the passive devices are fully utilized [9-10].

Due to the excellent performance of LLC resonant converter, LLC resonant converter has attracted wide attention since its proposed date. Especially since 2003, scholars at home and abroad have done a lot of research on LLC resonant transform topology, including the application and design optimization of the LLC circuit principle in the DC/DC power supply module [11-13], the advantages of the application of the LLC converter and the detailed analysis of the large changes in the input voltage and load [14-16].

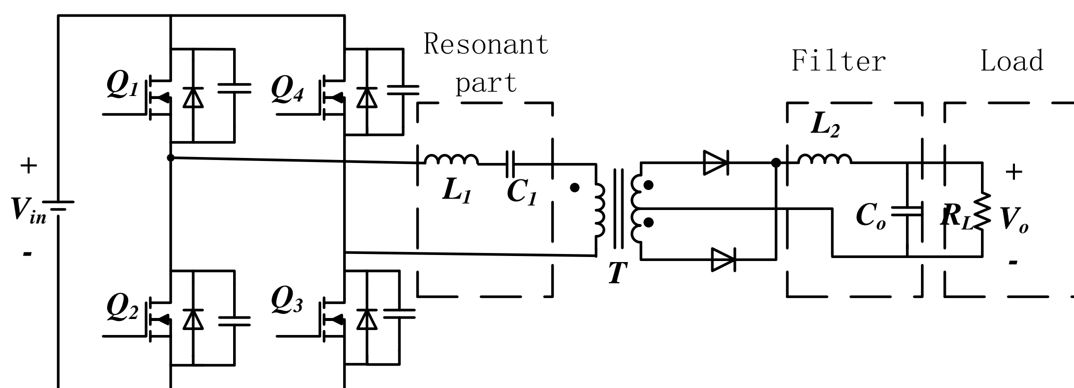

Figure 1-4 Structure of resonant converter network

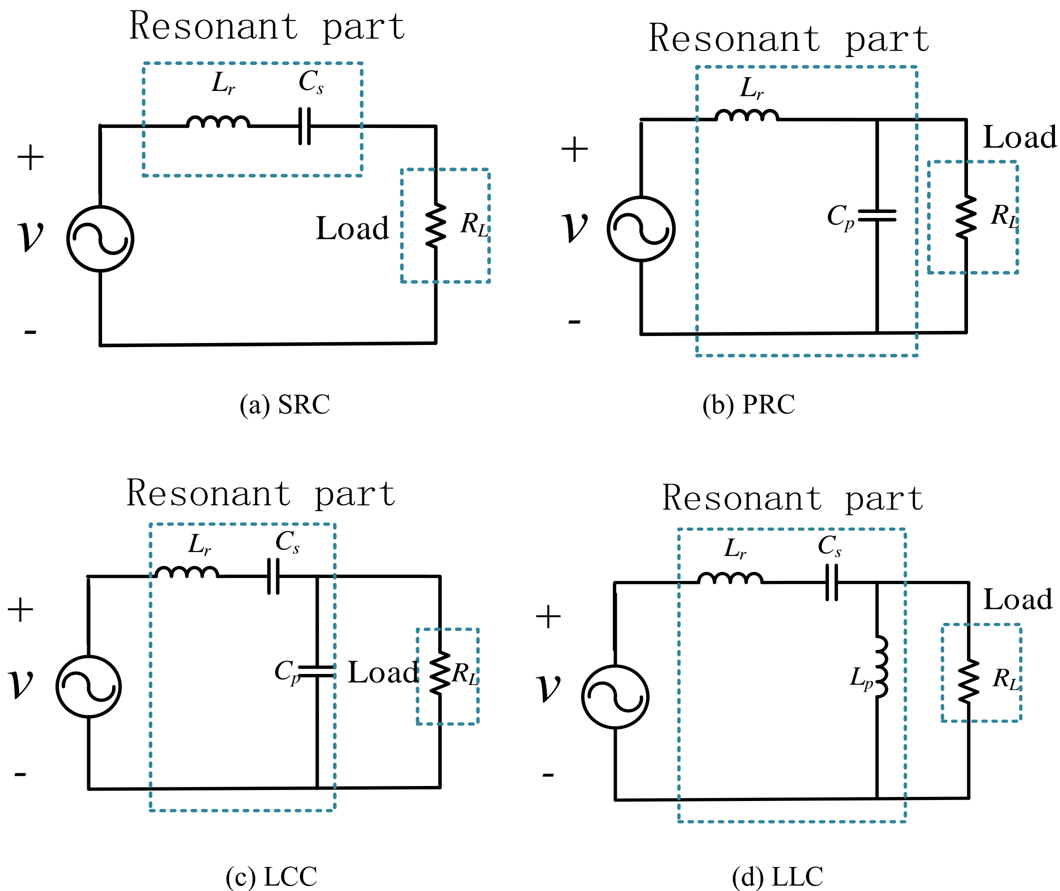

Figure 1-5 Diagrams of equivalent circuit

The first generation of semiconductors is a semiconductor material represented by silicon (Si) and germanium (Ge), which is widely used in the fields of electronics and circuits, and plays an important role in the development of the electronic information industry. The second generation semiconductor materials are mainly compound semiconductor materials represented by InSb and GaAs. These materials are mainly used in the manufacture of high frequency electronic devices and luminescent electronic components. The third generation semiconductor materials are the wide band gap semiconductor material represented by GaN and SiC [17-18]. In the field of power supply, the structure design and manufacturing process of silicon power devices have been improved in the recent decades. The performance of silicon devices has been close to the theoretical limit of its material characteristics, and the lifting space is very small. In order to further improve the performance of the power module, more and more power and electronic devices experts have shifted their attention to the third generation wide band gap semiconductor materials. They widely studied and paid attention to the third generation of semiconductor materials represented by silicon carbide (SiC) and

gallium nitride (GaN) [19]. The material properties of silicon, silicon carbide and gallium nitride are as follows:

Table 1-1 Material properties of silicon, silicon carbide and gallium nitride [20]

Parameter	Si	SiC	GaN
Band gap energy EG/eV	1.12	3.2	3.39
Critical breakdown electric field $E_{BR}/MV\cdot cm^{-1}$	0.3	3.5	3.3
Saturation drift velocity $Vs/\times 10^7 cm\cdot s^{-1}$	1.0	2.0	2.5
Electron mobility $\mu/cm^2\cdot V^{-1}\cdot s^{-1}$	1500	650	900~2000
Thermal conductivity λ/W·cm-1·K-1	1.5	4.5	2.2

From the table, we can see that the band gap energy of SiC and GaN is relatively high. The higher the band gap energy, the higher the withstand voltage of the material. In addition, the critical breakdown electric field of SiC and GaN is much higher than that of Si, which makes SiC and GaN possess good voltage withstanding characteristics. The higher GaN saturation drift velocity and electron mobility ensure that it is more suitable for working in high frequency. SiC and GaN have higher thermal conductivity, indicating that their thermal conductivity is excellent and can work at higher temperature [21].

However, there are some problems that we need to focus on in the research and application of GaN devices [22-24], such as:

1) The junction capacitance of gallium nitride devices and the gate driven charge are very small, which makes the device have a fast switching speed, but also makes the switching current which changes very rapidly during the switching process. It may cause the overvoltage of the switch device, and eventually causes the difference of electromagnetic interference, circuit error, device damage and so on.

2) Due to the low gate tolerance of the existing GaN HEMT devices, the normal noise tolerance is very small, and the parasitic oscillation of the gate drive circuit may also cause the misoperation of the circuit or the breakdown of the device.

3) In the application field of high current, it is usually necessary to parallel some GaN chips in order to reduce the conduction loss of the device. Due to the inevitable existence of parasitic inductors in the circuit, when the parasitic inductance of each device is inconsistent,

the current between the parallel devices will be unbalanced during the dynamic process. This leads to the problem of large loss and serious heat of individual devices. Finally, it limits the performance of the whole converter and increases the difficulty of the parallel connection of the switch tube.

4) At present, the size of the GaN device is very small, usually less than 1 square centimeters. And the electrode is drawn from the pad. The advantage is that the parasitic inductance can be reduced. But the shortcomings are also very obvious: because the chip has no heat dissipation substrate, the heat generated by the tube is carried to the PCB by the lead wire, and then emanated into the environment. The thermal resistance of these is very large. This determines that the heat dissipation of GaN devices totally is very bad and it is difficult to fully display their performance advantages.

These problems increase the difficulty of circuit design of GaN devices and seriously affect the application and promotion of GaN devices. In order to give full play to the performance advantage of GaN devices and reduce the difficulty of its application, the academic circles beGaN to study the integrated technology of GaN devices. We hope to solve the above problems through the integration of key components and provide a convenient and optimized solution for the application engineers.

In the application of high power density and high efficiency converters, GaN devices have better performance than Si devices [25]. The applications of early GaN devices are mainly focused on the topology of Buck, Boost converters and inverters [26-28]. In recent years, people beGaN to extend the research and application of GaN devices to new fields such as LLC converters. In detail, a lot of work has been done to analyze the switching process and loss characteristics of GaN devices and to give the corresponding loss models [29-30].

In order to further enhance the power density of the power module, it is usually possible to adopt the way of increasing the working frequency of the switching power supply. This can effectively reduce the volume of the converter's magnetic components, especially the transformer. The use of high density magnetic components can more effectively promote the high-frequency and miniaturization of module power supply [31]. Due to the obvious superiority of planar transformers in height, common high density magnetic components usually adopt planar variable structure. The typical planar transformer structure is shown in Figure 1-6. Planar transformers usually use ferrite materials suitable for high frequency

operation, so that their saturation magnetic flux is higher and iron core loss is lower. The flat structure is usually used to make the planar transformer have a larger contact area with the shell and radiator, which is beneficial to the heat dissipation of the transformer, the flat integration of the whole module and the increase of the power density. A flat winding or PCB winding can be used in the winding of a planar transformer, which makes it possible to ignore the effect of the skin effect and have a small AC resistance to reduce the copper loss [32]. The flat winding can also make the coupling between the primary side and the secondary side better, thereby reducing leakage inductance and corresponding loss, which is conducive to the improvement of efficiency [33-34].

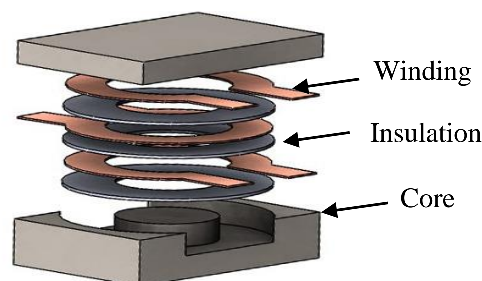

Figure 1-6 Planar transformer

With the increasing demand for the miniaturization of the converter, there are more and more researches on the planar transformer, including the analysis of the influence of the parasitic capacitance of the planar transformer on the performance of the transformer [35] and the optimization analysis of the design of the planar transformer for the secondary side synchronous rectifying tubes of the GaN devices [36]. The researchers, led by Professor Lee FC, have made a further analysis and optimization of the loss of the plane transformer, especially the iron loss, by using a matrix transformer [37-39].

The conventional isolated DC/DC converter usually uses diodes as rectifier in the secondary side. However, there is a large turn-on voltage drop when the diode is switched on. A large conduction loss is generated when flowing through a large current, which seriously reduces the efficiency of the converter. Synchronous rectification technology is a scheme for reducing diode loss [40]. In the rectifier part, the switch is used to replace the original diode, and the corresponding synchronous switching signal is provided. Because the switching loss is small, the turn-on loss and the turn-off loss can make use of the reasonable driving signal

to realize ZVS/ZCS [41-42]. So the loss of the rectifier can be greatly reduced. If the LLC resonant converter does not work at the resonant frequency, the influence of the parasitic inductance and the resistance of the switch tube must be taken into consideration [43].

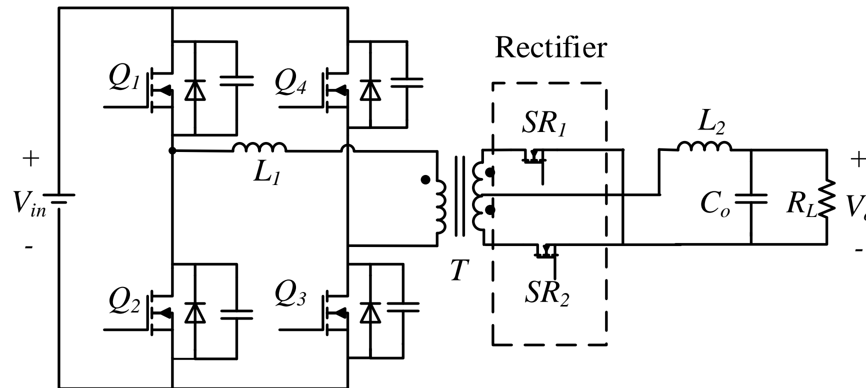

Figure 1-7 Diagram of synchronous rectification

In order to further satisfy the performance of power supply with stable and low consumption, more and more researches on synchronous rectification have been made in recent years, and various detailed modulation schemes have been put forward. After understanding the change of the driving signal and current in each phase of the synchronous rectifier [44], a variety of control methods, including angle modulation, coordinate modulation, digital control and predictive modulation, can be used for synchronous rectification [45-48].

Due to the wide application of various technologies, high power density products on the market have also emerged in recent years. At present, the main producers of high-power density power in the world are SynQor and Vicor. Figure 1-8 is the two DC/DC power converters produced by SynQor company. Figure 1-9 is the two DC/DC power converters produced by Vicor company. Table 1-2 is their main parameter.

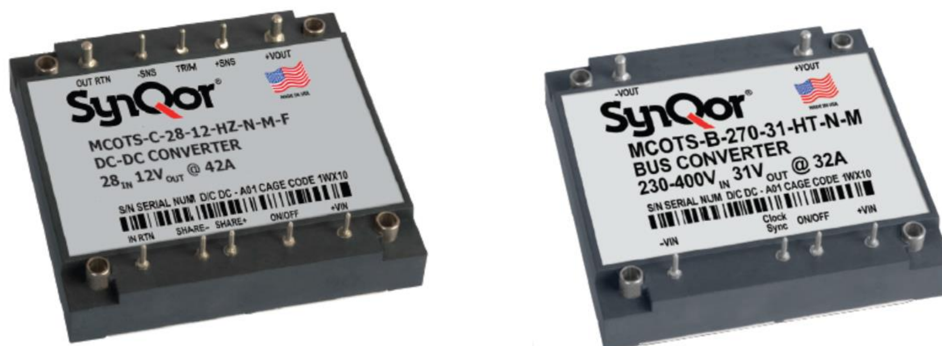

（a）28V/12V 200W DC/DC converter （b）270V/31V 1000W DC/DC converter

Figure 1-8 Converters produced by SynQor

（a）48V/12V 300W DC/DC converter （b）384V/48V 800W DC/DC converter

Figure 1-9 Converters produced by Vicor company

Table 1-2 Main parameter of high power density converters

Product	**MCOTS-C-28V-12-HZ**	**MCOTS-B-270-31-HT**	**VTM48EF120M025A00**	**BCM6123TD1E5117Tzz**
Producer	SynQor	SynQor	VICOR	VICOR
Input voltage/V	28	270	48	384
Output voltage/V	12	31	12	48
Power/W	250	1000	300	800
Efficiency	91%	95%	96%	96%
Size/in^3	2.49×2.39×0.51	2.39×2.49× 0.51	1.28×0.86×0.27	2.5×0.9×0.28
Power density/（W/in^3）	82.4	329.5	1009.4	1269.8
Tube type	MOSFET	MOSFET	MOSFET	MOSFET

At present, most of the power modules on the market use MOSFET as switch tube, and the products based on GaN devices are relatively rare. Their efficiency is about 91%~96%, and the power density is quite different due to different applications and different packaging styles. This provides reference and contrast for the design of this paper. The purpose of this paper is to design a power module using GaN as switch tube.

1.2 Design requirement

According to the above issues and the products on the market, a request is put forward as follow:

Table 1-3 Design paramters

Parameter	Value
Input voltage/V	270
Output voltage/V	28
Power/W	1000
Frequency/ MHz	1
Efficiency	95%
Power density/$W\cdot in^{-3}$	400

2 THE ANALYSIS OF LLC RESONANT CONVERTER

Because of the shortcomings of the traditional converter in voltage gain, working frequency and variable load, we improve the topology of the converter, and we can get the topology of LLC resonant transformation. By reasonably setting the resonant frequency and switching frequency of the converter, the zero voltage switch of the primary side and the zero current switch of the secondary side can be realized conveniently. It can be said that the LLC resonant converter is an ideal topology of the resonant converter. This chapter will introduce the working principle and characteristics of the LLC resonant converter in detail.

2.1 Analysis of the working process of LLC resonant converter

Diagram 2-1 is the the main circuit of the half bridge structure of LLC resonant converter. In the diagram, S_1 and S_2 are the upper arm switch tube and the lower arm switch tube of the primary half bridge of the transformer. SR_1 and SR_2 are the synchronous rectifier switches of the full wave rectifying circuit of the secondary side of the transformer. The resonant network is mainly composed of the excitation inductor Lm, the resonant inductance Lr and the resonant capacitor Cr, in which the leakage inductance can be supplied by the transformer. Thus the design of the magnetic integration is realized. It can reduce the quantity and volume of the magnetic element and reduce the volume of the converter. Of course, if necessary, external leakage can also be added.

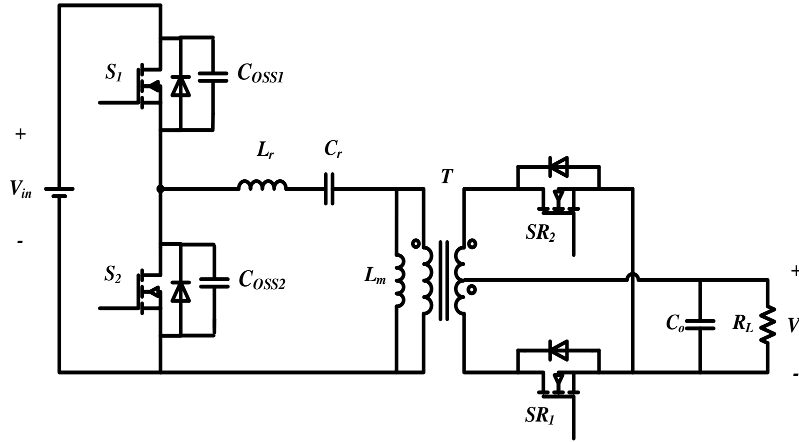

Figure 2-1 Diagram of LLC half-bridge converter

By analyzing the LLC resonant network, we can get the two resonant frequencies f_{r1} and f_{r2} of the topology. The expressions are as follows:

$$f_{r1} = \frac{1}{2\pi\sqrt{L_r \cdot C_r}} \qquad (2\text{-}1)$$

$$f_{r2} = \frac{1}{2\pi\sqrt{(L_r + L_m) \cdot C_r}} \qquad (2\text{-}2)$$

Where, f_{r1} - series resonant frequency /Hz; f_{r2} - series parallel resonant frequency /Hz; Lr - resonant inductance /H; Cr - resonant capacitance /F; Lm - excitation inductance /H.

According to the relationship between the operating frequency f_s of the converter and the series resonant frequency f_{r1} and the series parallel resonant frequency f_{r2}, the LLC resonant converter has three feasible working states: $f_{r2} < f_s < f_{r1}$, $f_s = f_{r1}$ and $f_s > f_{r1}$. When the $f_s < f_{r2}$, the impedance characteristic of the resonant network is capacitive and it is difficult to realize zero voltage switching of half bridge switch tube, so it is not analyzed and discussed [49]. The working process of the first three categories of work is analyzed below.

1) $f_s = f_{r1}$

The working frequency f_s is equal to the series resonant frequency f_{r1}, which is the ideal working state of the LLC resonant converter. The working waveforms of the LLC converter are shown in the figure:

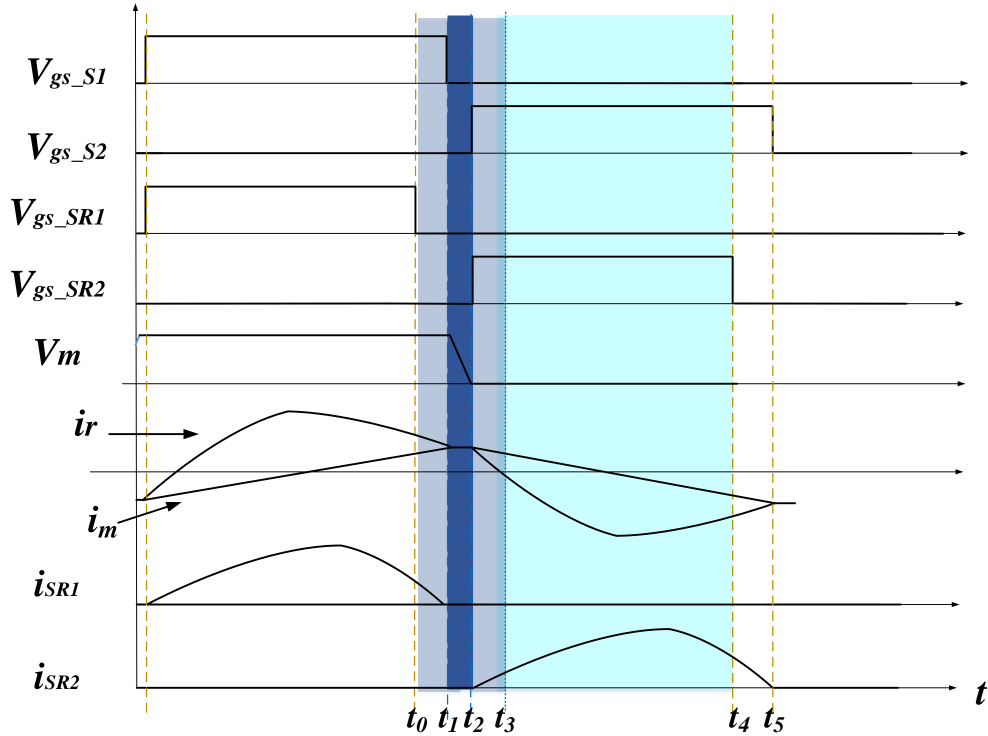

Figure 2-2 Diagram of LLC converter when $f_s = f_{r1}$

In the diagram, V_{gs_S1} and V_{gs_S2} are the driving voltages of the switch tube S_1 and S_2. V_{gs_SR1} and V_{gs_SR2} are the driving voltages of the synchronous tube SR_1 and SR_2. In order to ensure the reliability of the synchronous rectifier, the driving signal V_{gs_S1} and V_{gs_SR1}, the V_{gs_S2} and the V_{gs_SR2} exist a certain amount of time between the half bridge and the neutral point voltage of the primary half bridge of the transformer. The resonant current of the IM is the magnetizing inductance current of the transformer; i_{SR1} and i_{SR2} are the currents flowing through the synchronous rectifier SR_1 and SR_2.

In the [t_0~t_1] phase, the upper switch tube S_1 is on, and the lower switch S_2 is turned off. Because there is remainder between the primary side drive signal and the secondary side, the synchronous rectifying tube is turned off at the time of t_0. But the current i_{SR1} is still positive. And the current i_{SR1} passes through the body diode of the switch tube SR_1. If the frequency of the work is equal to the series resonant frequency, the switch tube S_1 is close at $i_r = i_m$. And the current passing to the secondary side through the transformer is zero, and the current passing of the secondary side is reduced to zero. The working loop at this stage is shown in the (a) stage of Figure 2-3.

In the [t_1~t_2] stage, the driving voltage of the primary side switch tube of the transformer is all low level, and S_1 and S_2 are all turned off to enter dead time. Due to the inductivity of the resonant network, the resonant current is still positive. The current flows through the S_2 body diode, discharging the output capacitance C_{0SS2} and charging the output capacitance C_{0SS1} of the S_1, which makes the neutral point voltage Vm decrease, and finally down to the reverse conduction voltage drop of the S_2 body diode. It can be seen that at t_2 time, the half bridge neutral point voltage V_m is changed from high voltage to low voltage. This process achieves commutation of thecurrent and prepares for soft switching of the next stage. Due to the short dead time, the amplitude of resonance current can be approximately invariable, and is equal to the peak value of excitation current. The working loop at this stage is shown in the (b) stage of Figure 2-3.

If the dead time is too long, the switch tube output capacitance charging and discharging have been finished, and the drain source voltage drops to zero. But the switch tube S_2 is still not open.The switch tube S_2 body diode will lead to the continuous flow in this time period, working circuit as shown in the diagram. However, the reverse conduction voltage drop of gallium nitride devices is much higher than that of silicon devices, resulting in a great loss of S_2 during this period and should be avoided as far as possible. Therefore, the dead time should be optimized in the actual application process, to reduce the reverse conduction time and reduce the corresponding loss. In this case, the current flow will appear as shown in the (c) stage in Figure 2-3.

In the [t_2~ t_3] phase, at t_2 time, Vm voltage drop to zero, at this time the V_{gs_S2} drive signal is high level, so S_2 turns on. Because the resonant network is inductive, the current flows through the network lag behind the voltage. The direction of the resonant current is invirable, still positive. As mentioned in the previous stage, the S_2 output capacitor C_{0SS2} discharge is exactly completed in the dead time, so the drain-source voltage of S_2 is close to zero, and the switch tube S_2 realizes zero voltage switching. Im and IR begin to decrease, but i_m>i_r, so i_p<0, i_{SR2}>0 on the secondary side of. As the tube SR_2 has achieved zero voltage, when the drive signal V_{gs_SR2} provides high voltage, current flows through the channel of SR_2, realizing zero voltage opening at the secondary side. The working loop at this stage is shown in the (d) stage of Figure 2-3.

In the [t_3 ~ t_4] phase, the resonant current of t_3 begins to increase in reverse direction after zero crossing. The direction of current flowing through S_2 changes. Other states are the same as the previous stage. The working loop at this stage is shown in the (E) stage of Figure 2-3.

The [t_4 ~ t_5] phase analysis is similar to that of the [t_0~t_1] phase analysis. After t_5, it enters the working state of the lower half cycle, and the whole is similar to the previous half cycle state. In the time period of the i_r>0, the input power supply is supplied to the converter to achieve energy conservation and balance.

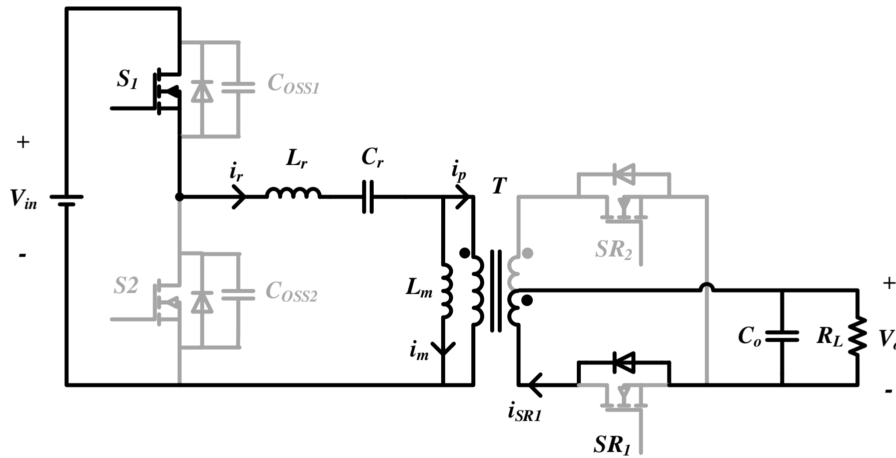

（a）[t_0~t_1]stage

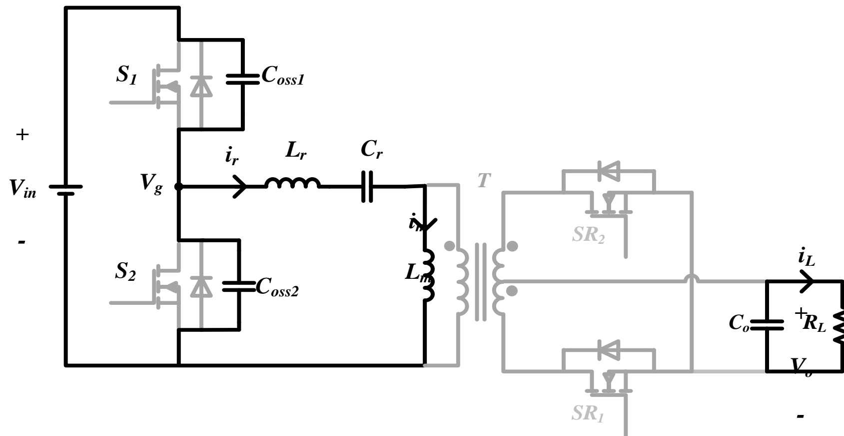

（b）[t_1~t_2]stageI

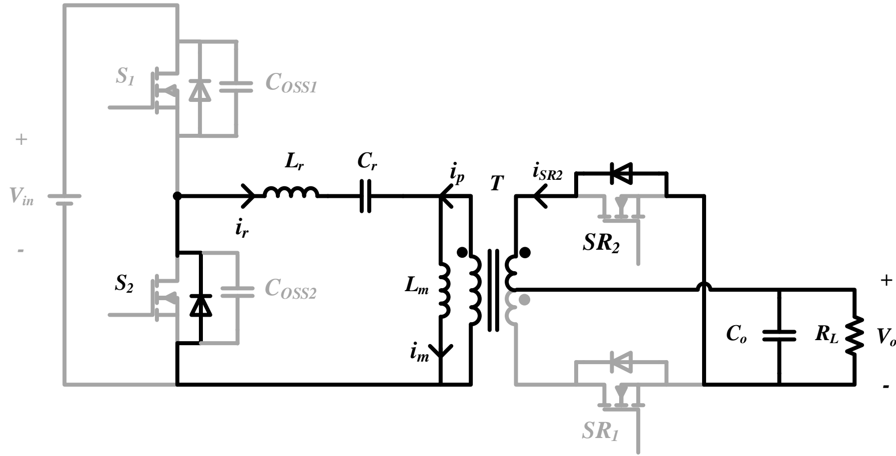

（c）[t_1~t_2]stageII

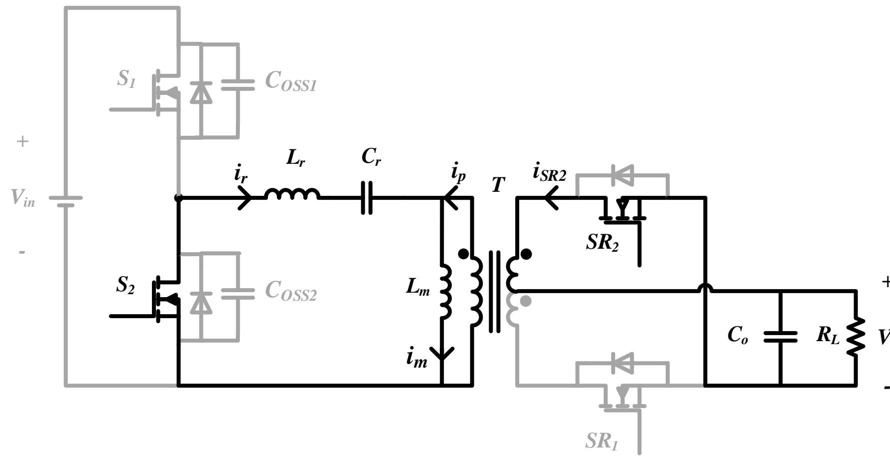

（d）[t_2~t_3]stage

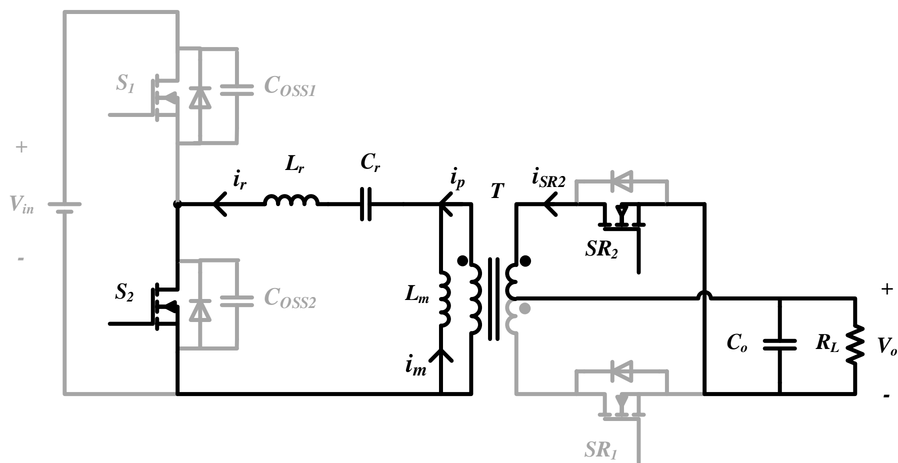

（e）[t_3~t_4]stage

Figure 2-3 Diagrams of switching process

2）$f_{r2} < f_s < f_{r1}$

When $f_{r2} < f_s < f_{r1}$, the working waveforms of the LLC converter are shown in the figure. Under this working condition, the working waveform is roughly similar to that of $f_s = f_{r1}$, but it needs to add a working stage [t_1~t_{10}].

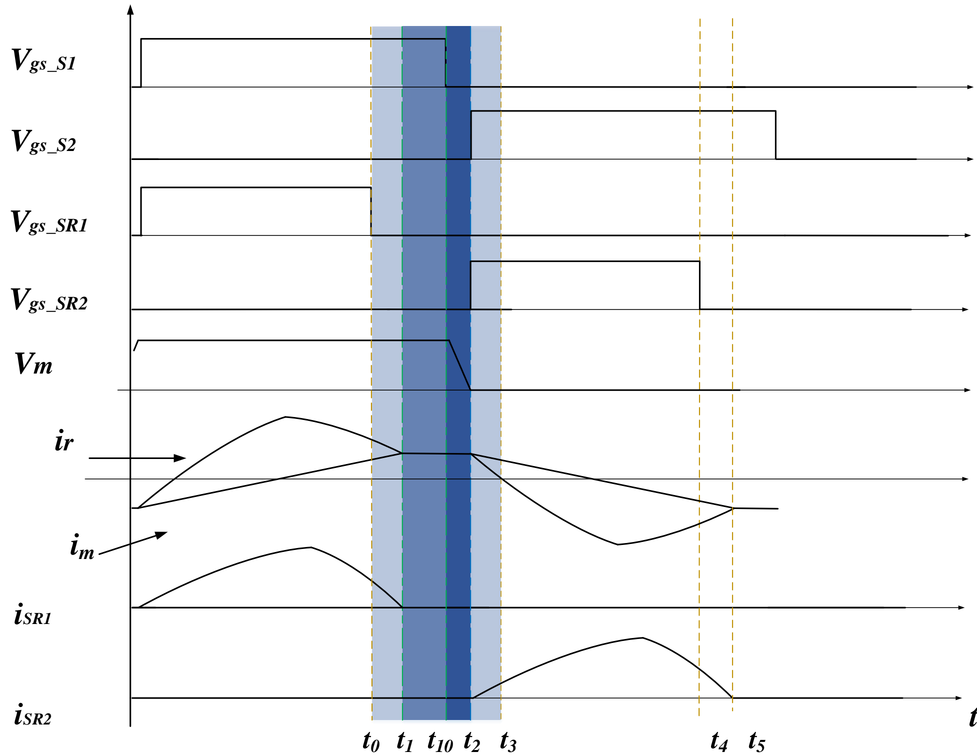

Figure 2-4 Diagram of LLC converter when $f_{r2} < f_s < f_{r1}$

In the [t_1~t_{10}] phase, the working frequency is less than the resonant frequency. When the resonant current is equal to the excitation current at t_{10}, the S_1 of the upper tube is still not turned off. At this time, the i_p drops to zero. The transformer no longer transfers energy to the secondary side, the secondary side current i_{SR1}which flows through the SR_1 become zero, and the load gets the energy from the output capacitor. This state is maintained until the switch S_1 turns off at t_2 and enters the next phase of [t_{10}~t_2]. The loop of this stage is shown in Figure 2-5.

But in this working state, the peak value of the resonant current will increase compared with the previous ideal state, and the circuit loss will increase due to the existence of the

conducting resistance, the equivalent resistance of the transformer and the equivalent resistance of the line.

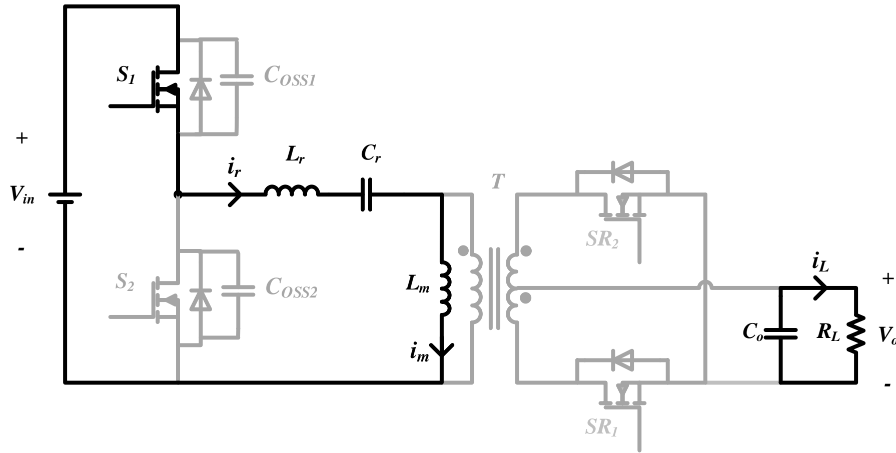

Figure 2-5 Diagram of current in [t_{10}~t_2]

3）$f_s > f_{r1}$

When $f_s > f_{r1}$, the working waveforms of the LLC converter are shown in Figure 2-6.

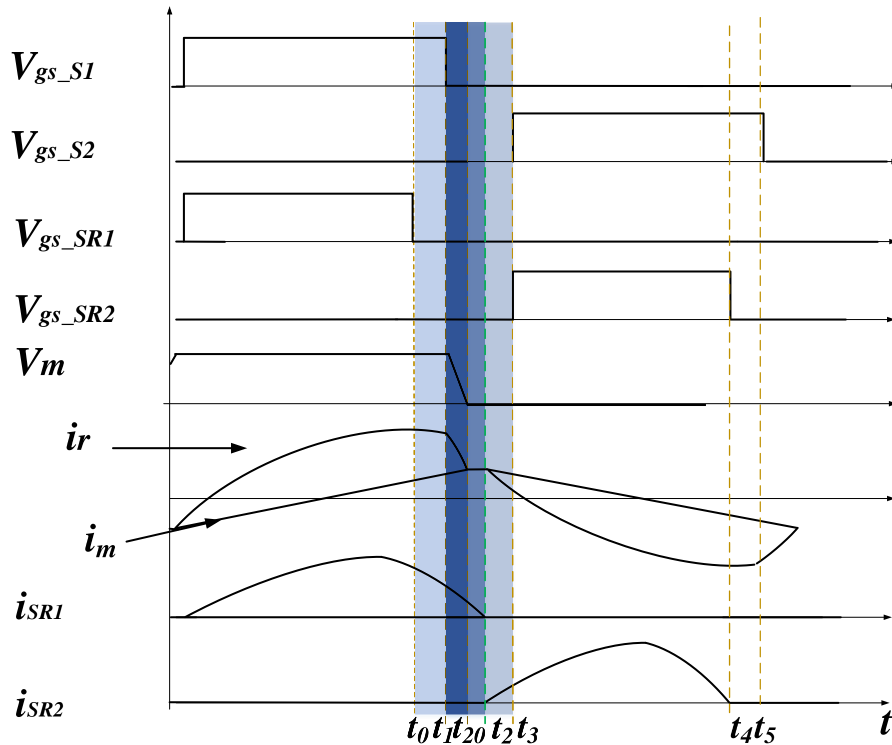

Figure 2-6 Diagram of LLC converter when $f_s > f_{r1}$

Compared with $f_s = f_{r1}$, the resonant current is not equal to the excitation current when switch tube is turned off at the primary side of the t_1 transformer, and the i_p is still positive. At this time, the primary side current flows through the body diode of the S_2. The secondary side current continues to flow through the body diode of the synchronous tube SR_1, and the converter works like [t_1~t_{20}] phase, as shown in Figure 2-7. At the moment t_{20}, the resonant current is equal to the excitation current, and the secondary side current of the SR_1 becomes zero. Due to the larger current change rate and the change rate crossing the zero point at this stage, the turn-off loss of the secondary side synchronous rectifier is larger, and it is difficult to realize the zero current switch of the LLC secondary side. The loop of this phase is shown in Figure 2-7.

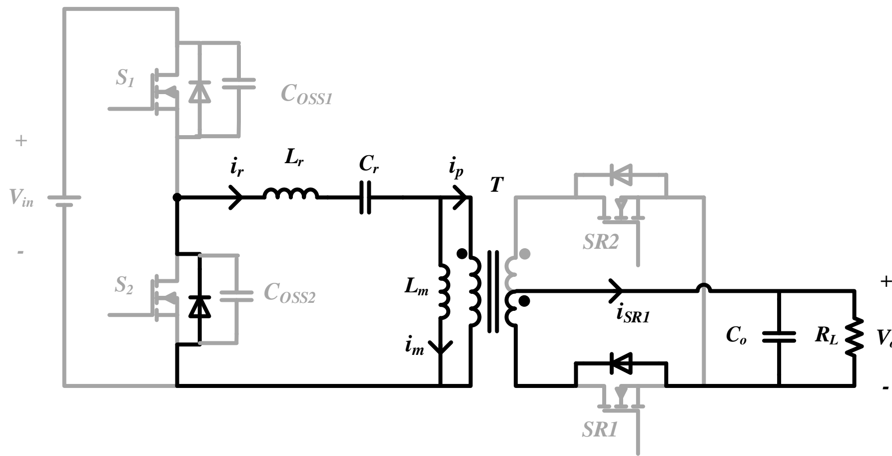

Figure 2-7 Diagram of current in [t_1~t_{20}]

2.2 Modeling of LLC resonant converter and DC gain characteristics analysis

The working principle of LLC converter has been known. We need to get the voltage gain expression of LLC circuit in order to accomplish the voltage transformation target. At this time, the first harmonic analysis (FHA) method is used, that is to use the first harmonic wave of square wave to replace the equivalent, ignoring the high order harmonic method for steady state modeling. So that the circuit is simplified, and the analysis is completed. Finally, we can the gain expression is obtained. Figure 2-8 is a simplified model comparison of the LLC resonant converter.

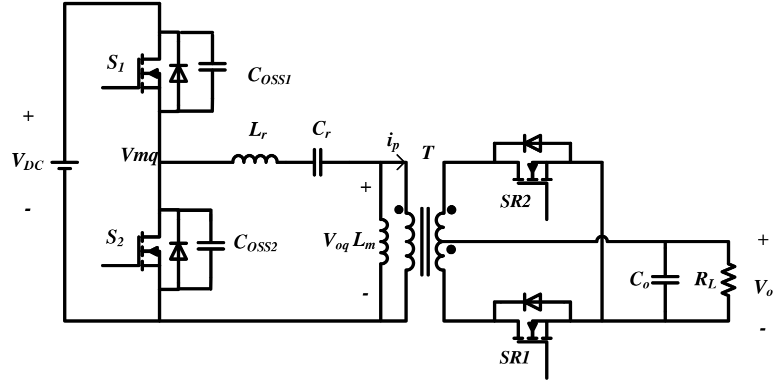

（a）Topology of LLC half-bridge converter

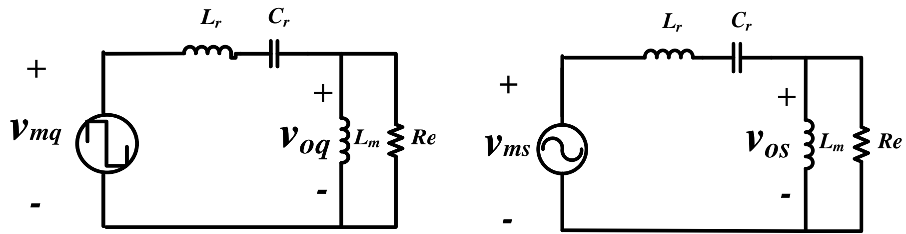

（b）Equivalent model for square wave （c）Equivalent model for sinusoidal wave

Figure 2-8 Topology and models of LLC resonant converter

In the figure, V_{DC} is the primary voltage of the transformer, V_{mq} is the half bridge neutral point potential, and the two are square wave. Fourier decomposition of V_{mq} is as follows:

$$v_{mq} = \frac{V_{DC}}{2} + \frac{2V_{DC}}{\pi} \sum_{n=1,3,5...} \frac{1}{n} V_{DC} \sin\left(n2\pi f_s t\right) \tag{2-3}$$

Ignoring the DC component and the higher harmonic component, the equation of the input voltage and the input current of the equivalent circuit of the LLC converter can be obtained.

$$v_{ms} = \frac{2}{\pi} V_{DC} \sin\left(2\pi f_s t\right) \tag{2-4}$$

$$i_{ac} = \frac{\pi}{2n} I_o \sin(2\pi f_s t) \tag{2-5}$$

Where,V_{DC} - transformer primary side voltage /V; f_s - switching frequency /Hz; I_o - output current average /A; n - transformer ratio.

Similarly, output voltage and output current can be obtained.

$$v_{os} = \frac{4}{\pi} n V_o \sin\left(2\pi f_s t - \phi_v\right) \tag{2-6}$$

$$i_{os} = \frac{\pi}{2n} I_0 \sin\left(2\pi f_s t - \phi_i\right) \tag{2-7}$$

Where, ϕ_v - phase difference of the primary side voltage of the transformer; ϕ_i - phase difference of the primary side current of the transformer.

According to equation (2-6) and (2-7), the equivalent output resistance is as follows:

$$R_e = \frac{v_{os}}{i_{os}} = \frac{8n^2}{\pi^2} R_L \tag{2-8}$$

The absolute value of the voltage gain is as follows:

$$|M| = \left|\frac{V_{os}}{V_{ms}}\right| = \frac{nV_o}{V_{DC}/2} = \left|\frac{(j2\pi f_s L_m) \,||\, R_e}{j2\pi f_s L_r + 1/j2\pi f_s C_r + (j2\pi f_s L_m) \,||\, R_e}\right|$$
$$= \left|\frac{1}{\sqrt{\left[1+\frac{1}{L_n}(1-\frac{1}{f_n^{\ 2}})\right]^2 + \left[Q\left(f_n - \frac{1}{f_n}\right)\right]^2}}\right| \tag{2-9}$$

Among them, the equation of normalized frequency FN, inductance ratio Ln and quality factor Q are as follows:

$$f_n = \frac{f_s}{f_{r1}} \tag{2-10}$$

$$L_n = \frac{L_m}{L_r} \tag{2-11}$$

$$Q = \frac{\sqrt{L_r / C_r}}{R_e} \tag{2-12}$$

Where, n - transformer turn ratio; f_s - switching frequency /Hz; f_{r1} for series resonant frequency /Hz; V_{DC} - input DC voltage /V; V_o - output DC voltage /V; I_o - output DC current average value /A; R_e - equivalent output resistance / Ω.

According to the previous equation (2-9) of voltage gain, the gain characteristic M of the converter and the normalized frequency f_n are mainly determined by the quality factor Q and the inductance ratio L_n. The gain characteristic diagram of the LLC resonant converter can be drawn from the equation (2-9), as shown in Figures 2-9 and 2-10. The inductor ratio is L_n=5 and L_n=15 respectively. Because this design is open loop control, in order to make the voltage gain be less affected by the load, the inductance ratio L_n should be larger than that in the FM control.

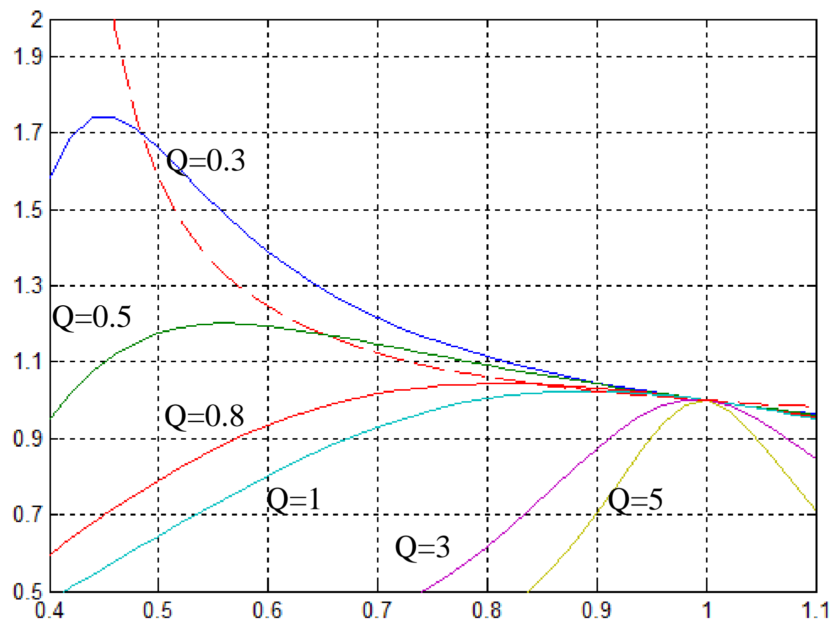

Figure 2-9 Gain curve of LLC resonant converter (L_n=5)

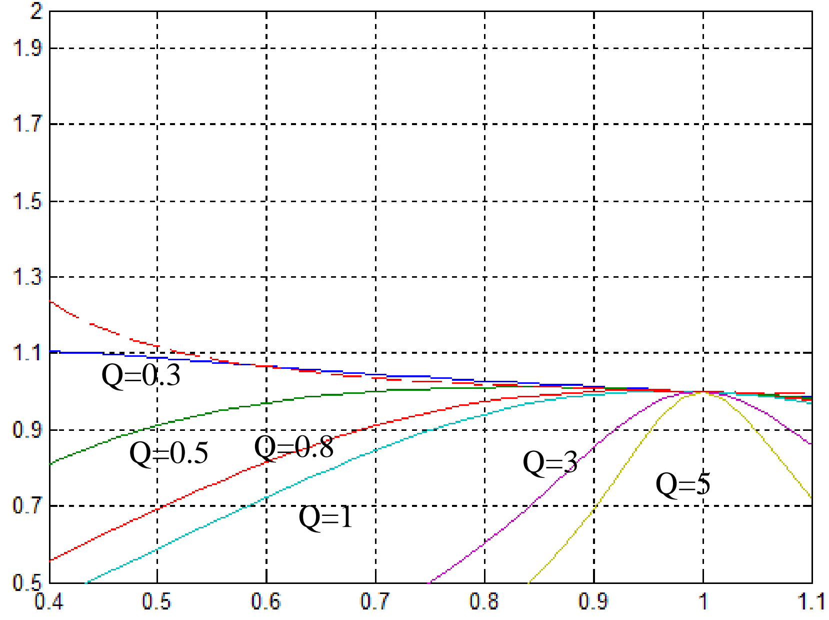

Figure 2-10 Gain curve of LLC resonant converter (L_n=15)

The input impedance of the fundamental equivalent model of the LLC resonant converter can be obtained as follows:

$$
\begin{aligned}
Z_e &= j\omega L_r + \frac{1}{j\omega C_r} + \frac{j\omega L_m \cdot R_e}{j\omega L_m + R_e} \\
&= \frac{R_e}{L_n^2 f_n^3 + \frac{f_n}{Q^2}} \left\{ L_n^2 f_n^3 + j\left[\frac{1}{Q} f_n^2 (1+L_n) - \frac{1}{Q} - L_n^2 Q\left(1-f_n^2\right) f_n^2 \right] \right\}
\end{aligned}
\quad (2\text{-}13)
$$

If the imaginary part of the input impedance is zero, the gain expression of the resonance network can be obtained when it is resistive.

$$
M_{res} = \frac{1}{\sqrt{\frac{1}{L_n}(1-\frac{1}{f_n^2})+1}} \quad (2\text{-}14)
$$

In the figure, the expression is the red dotted line. In the upper right part of the red dotted line, the circuit topology resonance network impedance is inductive. The resonant network current lag to the voltage, so it is the ZVS region of the gain network. In the lower left part of the red dotted line, the circuit topology resonant network is capacitive. The resonant network voltage lag to the current, and it is the ZCS region of the gain network. It is also found that, under different load conditions, the curve constant over (1,1) point, that is, when

the working frequency is FR1, the voltage gain of the resonant network is 1, not affected by the load. When the working frequency is slightly less than FR1, the voltage gain increases with the decrease of working frequency. The resonance network plays a boost role and works in the ZVS region. However, when the working frequency continues to decrease, the gain curve will pass through the ZVS area into the ZCS region, and the resonant network is capacitive and can not complete the ZVS of the switch tube. This is a process that must be avoided in design process.

To sum up, the working frequency of this design is equal to or slightly less than series resonant frequency.

2.3 Summary

In this chapter, the principle and process of the LLC converter are introduced in detail, and the voltage gain expression and image of the resonant network are given by using the first harmonic analysis method. The working state of the topology of the LLC circuit at different frequencies is analyzed in detail, and the range of the working frequency of the LLC converter is further determined. The analysis and conclusion of this chapter provide a theoretical basis for the parameter design of the LLC converter in the next chapter, and also provide theoretical guidance for the experiments.

3 CONVERTER DESIGN

The design of the LLC resonant converter topology is shown in Figure 3-1, and its parameters are shown in Table 3-1.

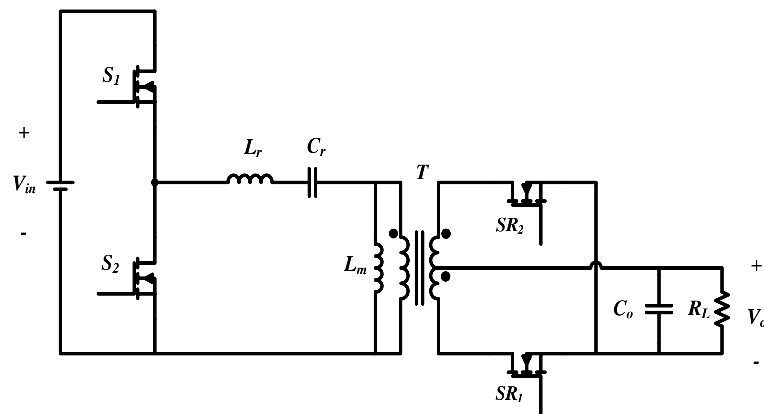

Figure 3-1 Topology of the converter

Table 3-1 Parameters of the converter

Parameter	Value
Input voltage/V	270
Output voltage/V	28
Power/W	1000
Frequency/ MHz	1

3.1 Design of main circuit parameters

As mentioned in the last chapter, in order to make the LLC converter working in the optimal working state, we make the converter working frequency equal to the series resonant frequency FR1, as shown in equation (3-1). At this time, the voltage gain is constant at 1 in

the full load range, so we can achieve the variable voltage requirements of the converter by controlling transformer ratio.

$$f_{r1} = f_s = \frac{1}{2\pi\sqrt{L_r C_r}} \tag{3-1}$$

Appropriate parameters play an important role in realizing the normal operation of the converter, realizing the ZVS of the switch, and ensuring the efficiency of the converter. Here, we need to determine the parameters of the converter's main circuit as the excitation inductor L_m, resonant inductor L_r and resonant capacitor C_r.

3.1.1 Design of magnetizing inductor

The selection of the excitation inductor L_m is not only related to the soft switching of the converter, but also to the current value of the original flow through the switch tube to a great extent, thus affecting the efficiency.

First, the excitation inductance affects the efficiency of the converter. In the converter, the conduction loss and switching loss of the switch tube, the copper loss of the transformer and the line loss are directly proportional to the current effective value. The primary and secondary side currents are all related to excitation inductance L_m when load and voltage ratio have been determined. Therefore, the larger the L_m, the smaller the effective value of the current flowing through the switch tube and the transformer, and the smaller the overall loss, thus improving the overall efficiency of the converter.

However, simply increasing the excitation inductance Lm is not desirable.

Through the analysis of the second chapter, we know that the resonant current is approximately equal to the peak of the excitation current at the turn-off moment of the primary switch tube, and the primaryl side voltage of the transformer is clamped, and the peak current peak can be obtained as shown by the equation. In the dead time, the charge discharge current i_m of the primary side switch capacitor C_{0SS} can be determined by the output voltage V_o, the transformer ratio *n* and the excitation inductance L_m. The charge relationship between charge and discharge can be determined by equation (3-2) and (3-3).

$$I_m = \frac{nV_o}{4L_m}T \tag{3-2}$$

$$2C_{0SS}V_{DC} \leq I_m t_d \tag{3-3}$$

Where, T - switching period /s; C_{0SS} - switch tube output capacitance /F; t_d - dead time /s.

For example of GS66508T, the relationship between the junction capacitance and the bearing voltage in the primary is shown in Figure 3-2. Here we need the equivalent output capacitance of the switch tube from 0V to 270V, and the value of C_{0SS} can be obtained by the curve (C_{0SS}) shown in Figure 3-2.

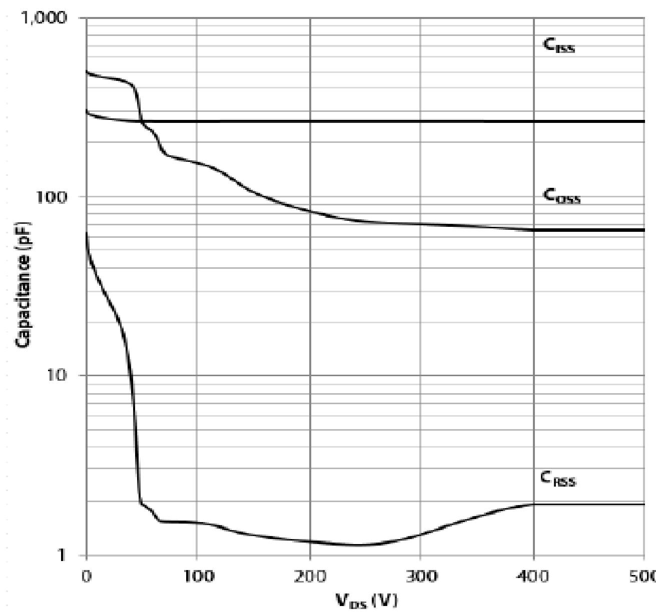

Figure 3-2 GS66508T capacitance characteristics

It can be seen that Lm has a minimum value to ensure zero voltage switching of the primary side.

Based on the above analysis, if the primary side switch is GS66508T, the equation of excitation inductance is as follows.：

$$\begin{aligned} L_m &= \frac{t_d}{16C_{oss}f_s} \\ &= 17.8(\mu H) \end{aligned} \tag{3-4}$$

3.1.2 Design of resonant inductor

The resonant inductance value is related to the maximum gain range of the converter. In practical applications, there is always a certain fluctuation in the input voltage side of the converter. If the output voltage is required to remain constant during the fluctuation, a suitable resonant inductance value is needed to meet the requirement of the voltage gain.

The relationship between inductance ratio Ln and quality factor Q is deduced from equations (2-10), (2-11) and (2-12).

$$L_n Q = \frac{2\pi f_{r1} L_m}{R_e} \tag{3-5}$$

In freuency modulation control loop, L_n is 3~8 based on experience. Because of the lack of frequency modulation control in this design, the inductance ratio of Ln should be much larger for f the effect of reducing the change of load on the voltage gain and output voltage. In this way, the magnetic integration can be completed flexibly according to the situation of the actual transformer, and the applied magnetic parts are avoided. It is beneficial to reduce the volume of the converter magnetic parts and improve the power density.

3.1.3 Design of resonant capacitor

Because the resonant capacitor Cr and the resonant inductor L_n jointly determine the series resonant frequency f_{r1}. The series resonant frequency and the excitation inductor are determined according to the previous article. So the resonant capacitance can be obtained directly. The equation is as follows：

$$C_r = \frac{1}{(2\pi f_s)^2 L_r} \tag{3-6}$$

3.2 Device selection

Assuming that the switching frequency of LLC circuit is equal to the series resonant frequency, the instantaneous value of resonant current and exciting current is expressed as follows.：

$$i_r(t) = \sqrt{2} I_{rms_p} \sin(\omega_0 t + \phi) \tag{3-7}$$

$$i_m(t)=\begin{cases}-\dfrac{nV_0T}{4L_m}+\dfrac{nV_0}{L_m}t & 0<t<\dfrac{T}{2}\\ \dfrac{nV_0T}{4L_m}-\dfrac{nV_0}{L_m}\left(t-\dfrac{T}{2}\right) & \dfrac{T}{2}<t<T\end{cases} \tag{3-8}$$

Where, φ-the initial phase angle of resonant current; I_{rms_p} - the effective value of resonance current /A; T - switching period /s.

The effective value of the primary resonant current can be got:

$$\begin{aligned}I_{rms_p}&=\frac{1}{8}\cdot\frac{V_0}{nR_L}\sqrt{\frac{2n^4R_L{}^2T^2}{L_m{}^2}+8\pi^2}\\&=8.2(A)\end{aligned} \tag{3-9}$$

The effective value of the secondary resonant current can be got:

$$\begin{aligned}I_{rms_s}&=\sqrt{\frac{1}{T}\int_0^{\frac{T}{2}}n\left(i_r(t)-i_m(t)\right)dt}\\&=\frac{1}{4}\cdot\frac{V_0}{R_L}\sqrt{\frac{5\pi^2-48}{12\pi^2}\cdot\frac{n^4R_L{}^2T^2}{L_m{}^2}+1}\\&=39.6(A)\end{aligned} \tag{3-10}$$

The peak value of the primary resonant current can be got as follows:

$$\begin{aligned}I_{peak_p}&=\sqrt{2}I_{\mathrm{rms}_p}\\&=11.6(A)\end{aligned} \tag{3-11}$$

The peak value of the secondary resonant current can be got as follows:

$$\begin{aligned}I_{peak_s}&=\sqrt{2}I_{\mathrm{rms}_s}\\&=56.1(A)\end{aligned} \tag{3-12}$$

3.2.1 Selection of primary side device

The voltage of the primary side should be 270V, while the voltage level of the GaN high voltage device is greater than or equal to 600V.

At present, GaN devices mainly come from GaN Systems, Efficient Power Conversion, (EPC) and Infineon, these three companies.

Because of the limited selection of high voltage GaN devices on the market, it is mainly the 650V series of GaN Systems company. Considering the conduction loss, output junction capacitance and price of the switch tube, this design initially uses transistor GS66508T as the primaryl side switch. The type of switch tube leakage source voltage, leakage current and working frequency meet the design requirements. And the resistance is small, which is beneficial to reduce the loss and improve efficiency. Its small volume is conducive to increasing the power density. The thermal resistance is small and the package design is the top heat dissipation, which is conducive to further cooling design.

Table 3-2 Parameters of GS66508T

Product	GS66508T
Productor	GaN Systems
V_{ds}/V	650
I_D/A (T_{case}=100 °C)	25
$R_{DS(ON)}$/mΩ(T_{case}=25 °C)	50
Q_G/nC	5.8
Size/mm×mm×mm	6.9×4.5×0.54
Thermal resistance (junction-to-case)/ °C /W	0.5

After the selection of the primary switch tube is completed, the loss of the primary side switch tube needs to be calculated.

1)Switching loss

Switching loss includes turn-on loss and turn-off loss. It is mainly caused by the overlap of the drain voltage and the current in the power switch. From the analysis of the second chapter, the LLC converter can realize the zero voltage switching of the primaryl side in the full load range, so the actual turn-on loss can be ignored. Here we only consider the calculation of the turn-off loss. The switching process of GaN devices is very complex. Most of the existing models are only suitable for Si devices. In order to obtain more accurate turn-off loss, this paper is based on the LTspice simulation model of GaN device GS66508T provided by GaN

L_3

Systems company, and uses LTspice circuit simulation software to simulate the voltage and current waveform during the shutdown of GaN device under the LLC resonant converter. Then turn-off loss of the switching device can be get by integrating the product of the voltage and current values. The results of waveform are as follows:

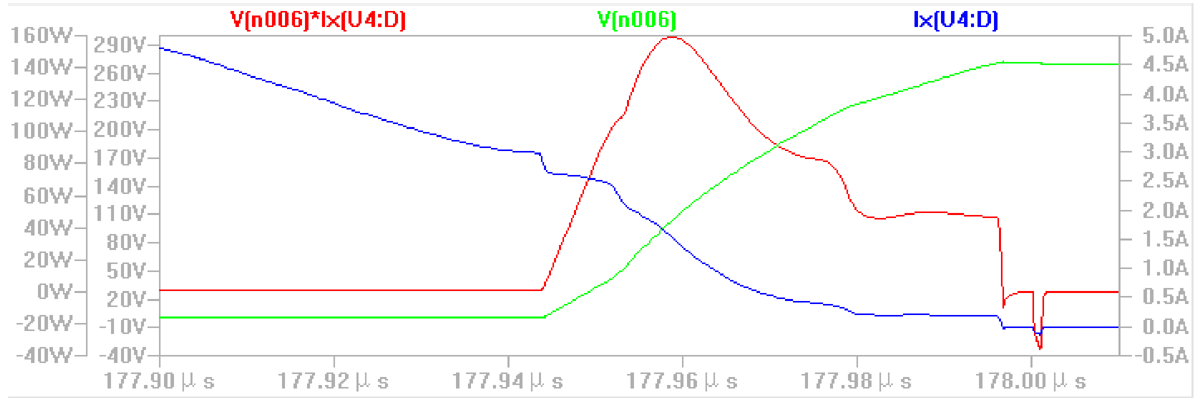

Figure 3-3 Voltage and current waveform of GaN when turned off

The blue curve L_1 in the picture is the half bridge neutral point voltage, that is the turn-off voltage waveform of the lower tube. The green curve L_2 is the current waveform when the tube is turned off. The red curve L_3 is the power waveform. Therefore, the turn-off loss of single switch tube can be obtained.

$$P_{off} = \int v(t) i\left(t\right) \mathrm{d}t \times f \tag{3-13}$$

The turn-off loss of single switch tube is calculated by simulation integral calculation. That is P_{off}= 0.73W.

2）Conduction loss

The conduction loss is the loss caused by current flowing through the switch tube during conduction. It is mainly related to the drain-to-source on resistance ($R_{DS（ON）}$) of the switch and the current RMS mentioned above. The relationship between $R_{DS（ON）}$ and temperature is very close, and its relation is given in Figure 3-4. In order to ensure the normal operation of the converter, the $R_{DS（ON）}$ of the switch tube at 100°C is chosen as the reference value.

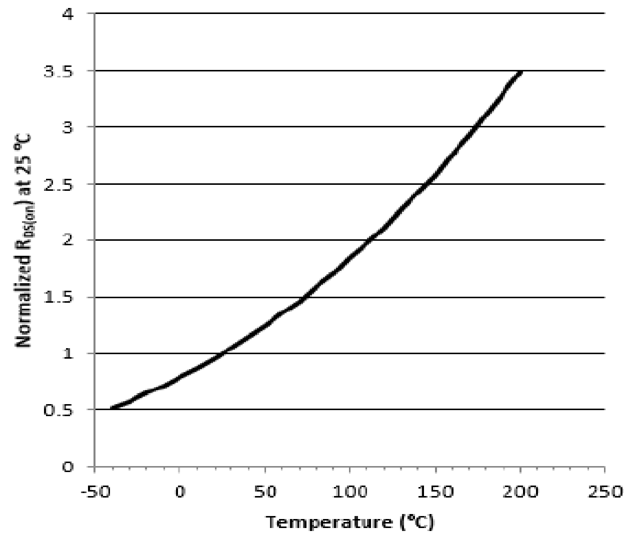

Figure 3-4 Relationship between $R_{DS(ON)}$ of GS66508T and temperature

According to the GS66508T data sheet, the $R_{DS(ON)}$ is 50Ω at 25 ℃. $R_{DS(ON)}$ =90Ω can be obtained at 100°C, and the conduction loss of single switch tube is calculated as follows:

$$\begin{aligned} P_{on} &= \frac{1}{2} I_{rms_p}{}^{2} \times R_{ds_on} \\ &= 0.5 \times 8.2^{2} \times 0.09 \\ &= 3.03(\mathrm{W}) \end{aligned} \tag{3-14}$$

3）Driving loss

In the process of turning on and turning off, the converter drive circuit charges and discharge. Therefore, the driving loss of the switch tube can be expressed as:

$$P_{dri} = Q_G \times V_{DD} \times f_s \tag{3-15}$$

Where, Q_G - the total charge of /C flowing through the gate; V_{DD} -- driving voltage /V.

According to the device manual, the gate charge of GS66508T is Q_G = 5.8nC, and the primary side drive voltage is V_{DD} = 6V. So the driving loss of the primary side switch tube is P_{dri} = 0.04W.

The total loss of single GaN devices on the primary side of the LLC resonant converter can be obtained from the above analysis.

$$\begin{aligned} P_{p1} &= P_{on} + P_{off} + \mathrm{P}_{\mathrm{dri}} \\ &= 3.03 + 0.73 + 0.04 \\ &= 3.8(\mathrm{W}) \end{aligned} \tag{3-16}$$

The total loss of the primary switches can be obtained.

$$\begin{aligned} P_p &= 2 \times P_{p1} \\ &= 2 \times 3.8 \\ &= 7.6(\mathrm{W}) \end{aligned} \tag{3-17}$$

3.2.2 Selection of secondary side device

The voltage under the secondary side rectifying tube is：

$$\begin{aligned} V_{ds_max} &= 2V_0 \\ &= 56(\mathrm{V}) \end{aligned} \tag{3-18}$$

When the traditional rectifier circuit works, the diode has a higher conduction voltage drop, usually about 0.7V. When the current is large, the conduction loss on the diode is very large, which seriously affects the efficiency improvement. In this design, the GaN device with low conduction loss is used to instead of diode. This paper compares the two low voltage GaN devices between GaN Systems and EPC. The main parameters are shown in Table 3-3. Because the secondary side current is large and the influence of loss on efficiency is considered mainly, the resistance of switch tube becomes the main index of device selection. By comparing the parameters of GS61008T and EPC2032, EPC2032 is chosen as the secondary side synchronous rectifier.

Table 3-3 Parameters of 100V GaN devices

Product	GS61008T	EPC2032
Producer	GaN Systems	EPC
V_{ds}/V	100	100
ID/A (T_{case}=25 °C)	90	48
$R_{DS(ON)}$ /mΩ(Tcase=25 °C)	7	3
QG/nC	12	12
Size/mm×mm×mm	7×4×0.54	4.6×2.6×0.79
Thermal resistance (junction-to-case)/ °C /W	0.55	0.45

The effective value and the peak value of the secondary current are respectively:

$$I_{rms_s} = 39.6(\text{A}) \tag{3-19}$$

$$I_{peak_s} = 56.1(\text{A}) \tag{3-20}$$

It is written in consideration of the loss of the secondary switch. Because the secondary side is synchronous rectification, the voltage has been reduced to zero at the time of tuening on. When turning off, the secondary side switch tube can realize ZCS, so the secondary side switch tube does not need to consider switching loss. However, because there is a certain amount of time between the secondary driving signal and the primary side signal when the synchronous rectifying tube is turned off, its waveform is shown in Figure 3-5. So the secondary side switch tube has the reverse conduction in the margin time. This part of the loss is large, and detailed calculations will be made in this section.

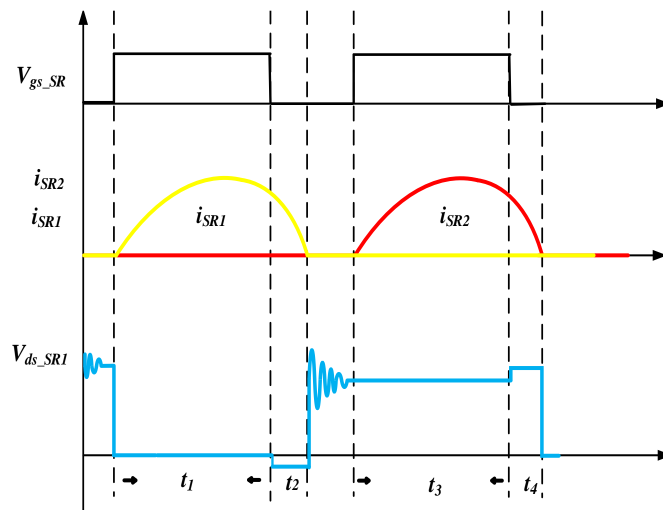

Figure 3-5 Diagram of synchronous rectifying waveform in secondary side

1) Conduction loss

The EPC2032 of the EPC company is used as the rectifying tube on the secondary side. The relationship between the $R_{DS(ON)}$ and the temperature is shown in Figure 3-6. According to the EPC2032 data sheet, the conduction resistance of the single switch tube is calculated at 25°C,and $R_{DS(ON)}$ =3mΩ when $R_{DS(ON)}$ is 4.5 mΩ, which can be obtained at 100°C.

$$
\begin{aligned}
P_{on_S1} &= \frac{1}{2}\times(\frac{I_{rms_s}}{2})^2\times R_{DS(ON)} \\
&= \frac{1}{2}\times(\frac{39.6}{2})^2\times 0.0045 \\
&= 0.89(\mathrm{W})
\end{aligned} \tag{3-21}
$$

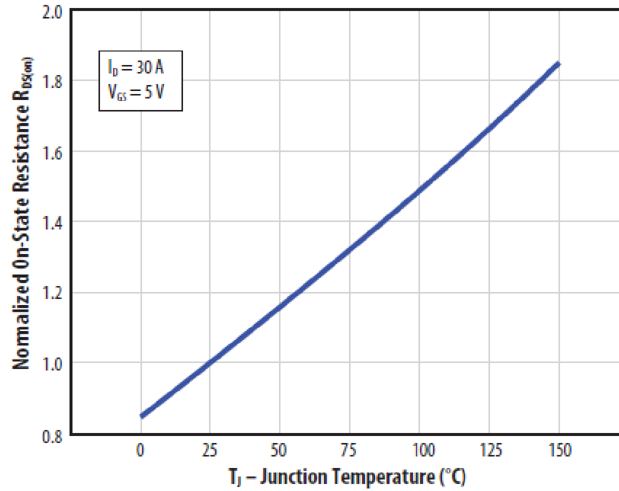

Figure 3-6 Relationship between $R_{DS(ON)}$ of EPC2032 and temperature

2）Reverse conduction loss

Due to the actual working process, the margin time of the side switch tube is very small in the whole switching cycle. The current waveform can be represented by the sinusoidal half wave at the peak value of I_{peak_s}, so one EPC2032 reverse conduction loss is:

$$
\begin{aligned}
P_{on_D} &= \int_{\frac{T}{2}-t_2}^{\frac{T}{2}} V_D \frac{I_{peak_s}}{2}\sin\left(2\pi f_s t\right)dt\times f_s \\
&= \int_{\frac{T}{2}-t_2}^{\frac{T}{2}} 2\times\frac{56.1}{2}\sin\left(2\pi f_s t\right)dt\times 1\times 10^6 \\
&\approx 0.68(\mathrm{W})
\end{aligned} \tag{3-22}
$$

3）Driving loss

The gate charge Q_g = 12nC can be found from the EPC2032 device data sheet. The driving voltage of the switch tube is V_{DD} = 5V. Substituting the equation (3-23) and calculating the drive loss of the secondary side rectifier tube:

$$\begin{aligned} P_{dri} &= Q_g \times V_{DD} \times f_s \\ &= 12\times10^{-9} \times 5\times1\times10^{6} \\ &= 0.06(\text{W}) \end{aligned} \tag{3-23}$$

The total loss of single synchronous tube on the secondary side of the LLC resonant converter can be obtained from the above analysis.

$$\begin{aligned} P_{s1} &= P_{on_S1} + P_{\text{on}_D} + P_{\text{dri}} \\ &= 0.89 + 0.68 + 0.06 \\ &= 1.63(\text{W}) \end{aligned} \tag{3-24}$$

Finally, the total loss of four switches on the secondary side can be obtained.

$$\begin{aligned} P_s &= 4\times P_{s1} \\ &= 4\times1.63 \\ &= 6.52(\text{W}) \end{aligned} \tag{3-25}$$

3.3 Main circuit simulation

Circuit simulation software LTspice is used to simulate the main circuit. The circuit simulation model is shown in Figure 3-7. The primary side switch uses the GS66508T LTspice simulation model provided by GaN Systems and the EPC2032 LTspice model provided by EPC. The driving waveforms of the switches are given by an independent voltage source $V_1 \sim V_4$. The L_1 and L_2 are the simulation of the leakage inductance of the secondary side of the transformer.

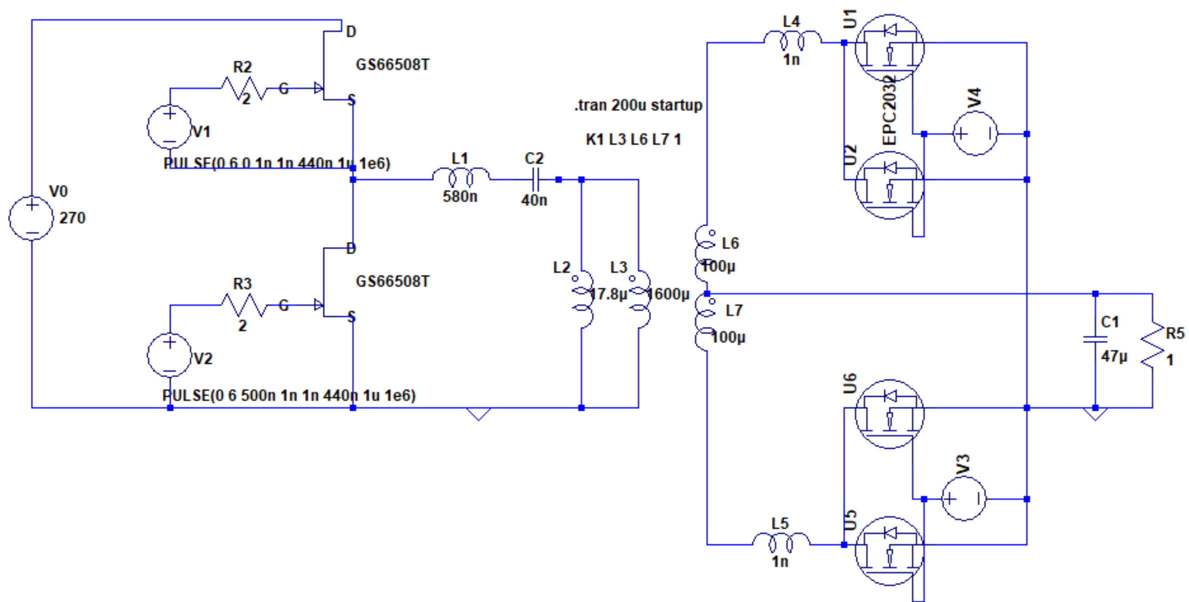

Figure 3-7 Circuit simulation model of LLC resonant converter

The simulation waveforms of the main circuit of the LLC resonant converter are shown in Figure 3-8. Figure 3-8 (a) is the primary side resonant current $I_{[L1]}$ (blue curve), the excitation inductance current $I_{[L2]}$ (red curve) and the neutral point voltage $V_{[n006]}$ (green curve) of the half bridge. The simulation results show that the circuit operates near the resonant frequency. The waveforms are basically consistent with the theoretical analysis. When the switch is turned off, the resonant current is slightly less than the excitation current because of the existence of the secondary synchronous rectifier switch, which has a larger output capacitance and parallel connection. Figure 3-8 (b) is the neutral point voltage $V_{[n006]}$ (green curve) and the current $Ix_{[U4:N]}$ (blue curve) of tube S_2. It can be seen that when the tube S2 is turned on, the voltage is approximately zero. It can be considered that zero voltage switching is realized on the primary side.

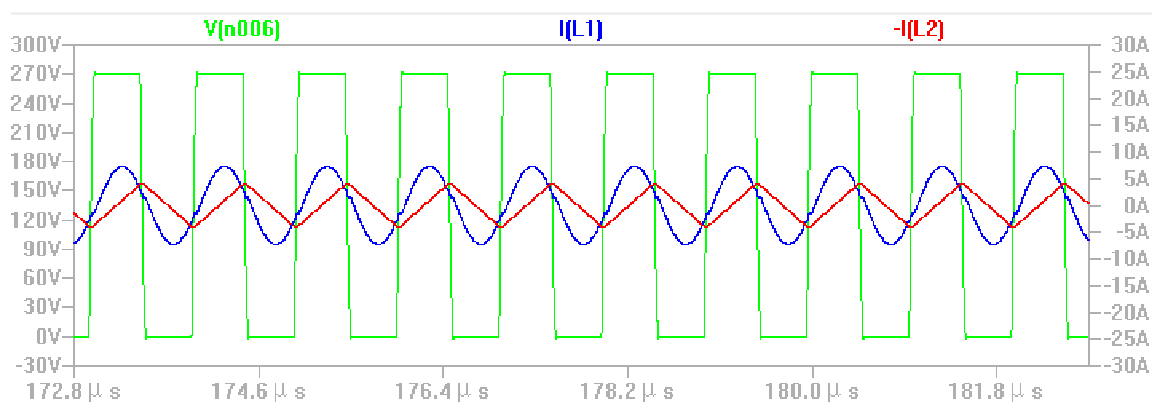

（a）LLC resonant waveform

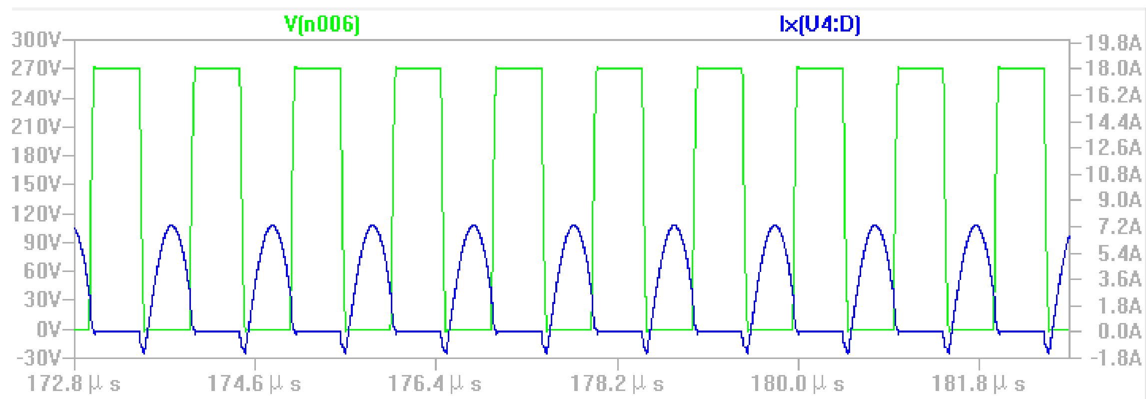

（b）ZVS waveform

Figure 3-8 LLC main circuit simulation waveform

3.4 Integrated and thermal design of converter

Making converters as a module is mainly related to its integrated design. The integrated design of the converter involves a series of problems such as the layout and cooling mode of the converter, the selection of PCB layers and the specific wire. A good integrated design can effectively guarantee the normal operation and stable performance of the converter. Finally, integrated design will also play an important role in the power density and loss of converters. At present, the size of GaN devices is very small, usually the electrode is led by the welding plate, which can reduce the area of PCB, also reduce the length of the lead and the parasitic inductance. But the shortcoming is also very obvious: (1) The thermal resistance of the device is very large. The chip size is small, and the chip has no heat dissipation substrate. The heat emission is all conduction to PCB, and then distributed through PCB to the environment, which leads to the large thermal resistance of the device. (2) The heat concentration problem. The chip size is small, and several GaN devices in the circuit must be reciprocated with each other to reduce loss of circuit parasitic inductance and power loop, resulting in heat concentration. The above two problems determine that the heat dissipation of GaN devices is very bad and it is difficult to fully display their performance advantages.

These problems increase the difficulty of circuit design of GaN devices and seriously affect the application and promotion of GaN devices. In order to give full play to the performance advantage of GaN devices and reduce the difficulty of its application, the researchers began to study the integration technology of GaN devices. People hope to solve the above problems

through the integration of key components, and provide a convenient and optimized solution for practical applications. In the circuit, People hope the key parasitic parameters of power circuit and driving circuit can be controlled simultaneously, and the drive design is optimized. Further, the heat dissipation of the device can be improved by adopting a high thermal conductivity cooling substrate.

3.4.1 Traditional structure design

The current converter structure, as shown in Figure 3-9, shows that the power device and other devices are on the same layer of printed circuit board with glass fiber epoxy resin (FR4) as the material. Because the thermal conductivity of FR4 is very small. It is only about 0.3W/m/K, so it is necessary to adhere small heatsinks to the top or bottom of the power device to assist the converter to dissipate the heat.

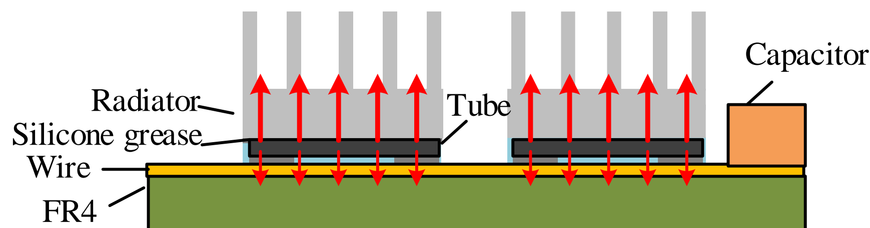

Figure 3-9 Diagram of traditional structure with FR4

This structure has the advantage of low cost and flexible assembly, so it is widely used as the most common converter structure. However, because the GaN device is usually small in size, especially the thickness is much thiner than the other components of the converter. It makes the radiator be not too large, usually less than 1 cubic centimeters, greatly limiting heat dissipation.

Figure 3-10 is a metal core printed circuit board (Metal Core PCB), in which the substrate is aluminum substrate, so it is also called PCB baced on aluminum substrate. When the insulating layer is rubber and ceramic particles, its thermal conductivity can reach 1~8W/m/K. But its disadvantage is that it can only be single layer wiring, which brings great difficulty to PCB wiring.

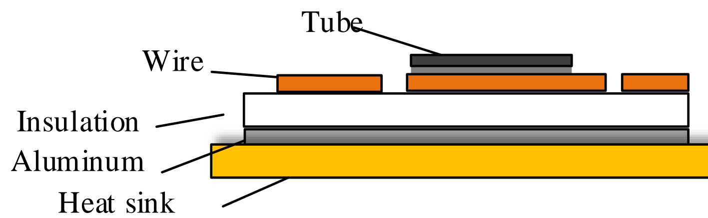

Figure 3-10 Diagram of the MCPCB

Figure 3-11 is a diagram of using direct bonding copper (DBC) as printed circuit board, where the insulating ceramic is made of aluminum nitride DBC and alumina DBC according to the material. The thermal conductivity and market price of the DBC board and the two front boards are shown in Table 3-4. By comparing FR4 materials, it is found that the thermal conductivity of DBC materials is high, but the price is high. And because of the limitation of technology level, the DBC currently processed on the market is mainly two layers, which can realize top and bottom layer wiring, not good as normal PCB board wiring.

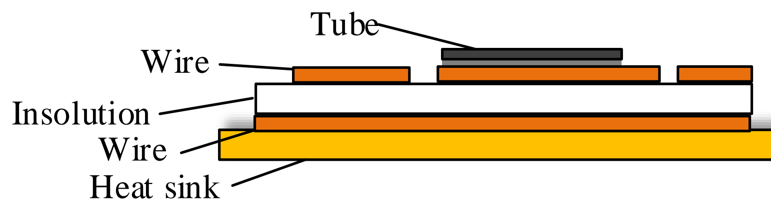

Figure 3-11 Diagram of DBC structure

Table 3-4 Comparison of various substrate parameters

Material	**Thermalconductivity （W/m/K）**	**Price(yuan/m^2）**
FR4	0.3	400~1000
DBC（AlN ）	180	80000~120000
DBC（ Al2O3 ）	25	30000~80000
MCPCB	1~8	7000~20000

Figure 3-12 shows a 650V/150A GaN half bridge power module. The module uses GaN Systems's enhanced GaN device. Due to the lack of busbar capacitors and drivers in the module, the parasitic inductance in the circuit is large, and the over voltage and oscillation problems are serious. The Fred C. Lee team of the US CPES has studied a half bridge power module of 600V/30mΩ GaN device, as shown in Figure 3-13. The module integrates busbar

capacitance, which can effectively reduce the parasitic inductance of power circuit. These modules weld GaN devices onto high thermal conductivity ceramic substrates and heat transfer from substrates. However, because the copper layer of the ceramic substrate is less and the wiring precision is poor, it is difficult to meet the requirements of the wiring process, such as the driving circuit.

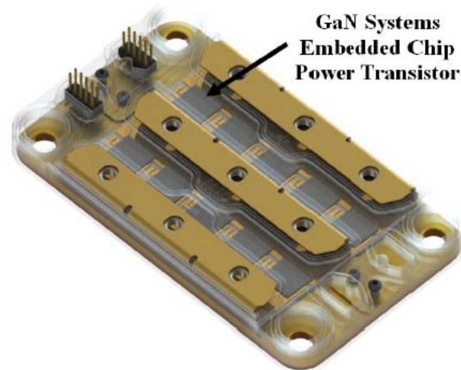

Figure 3-12 650V/150A half bridge power module of GaN device

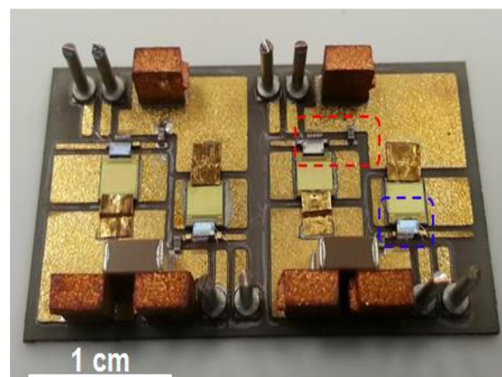

Figure 3-13 600V/30mΩ half bridge power module of GaN device

3.4.2 Optimized structure design

Considering that there is a certain gap between the structure mentioned above and the design requirement, a new structure is presented here, as shown in Figure 3-14. The substrate is PCB with FR4 material, which can realize multi-layer wiring and facilitate complex routing in small volume. In order to solve the heat dissipation problem, the power switch tube is placed at the bottom layer, which can transfer the heat generated by the power tube directly to the outer shell and the larger radiator. In order to further increase the heat dissipation, some copper foil with the same thickness as the switch tube can be arranged around the switch tube. The copper foil will direct the heat on the substrate into the radiator. And then fill the gap between the copper foil and the switch tube with the high thermal conductivity

of the silicone grease. Finally, the PCB substrate is connected with the radiator with the bolt to form a stable structure and ensure that the heat source of the switch tube and the transformer are in full contact with the radiator. In this way, the heat resistance of the heat source to the outside is as small as possible.

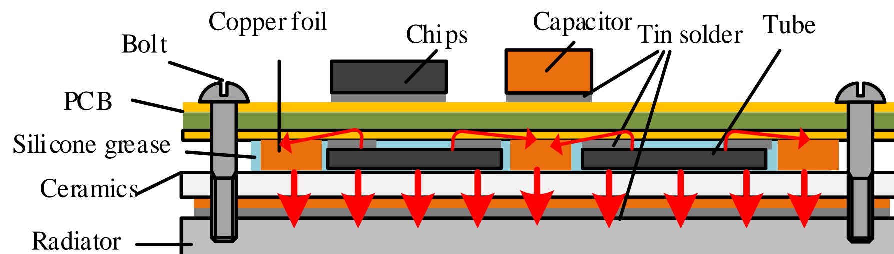

Figure 3-14 Diagram of optimized structure

Through such structural design, the advantages of PCB multi-layer wiring can be used to make the device distributed flexibly and ensure the reasonable optimization of its electrical parameters, such as the loop parasitic inductance mentioned in the following. Such a heat dissipation structure can also make the heat resistance of the switch tube to the radiator sufficiently small, which provides conditions for use of larger heat sink.

3.4.3 Thermal simulation of converter

FloTHERM is a software widely used by the global electronic system design engineer and electronic circuit design engineer to analyze the heat dissipation. The software has a large number of model libraries specially developed for the electronics industry. Its powerful solver has been developed and upgraded for electronic cooling applications for many years.

The heat dissipation effect of the above structure is simulated by the FloTHERM. The simulation model is shown in Figure 3-15. The primary side switch tube and the secondary side switch tube add the loss power according to the calculation results obtained by the 3.2 sections. The device designs the heat dissipation parameters according to the parameters of GS66508T and EPC2032. The simulation results are shown in Figure 3-16.

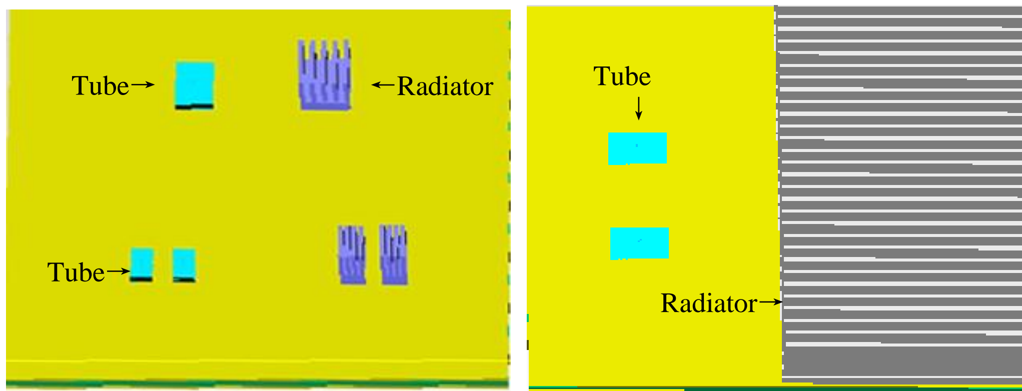

（a） Traditional structure （b） Optimized structure

Figure 3-15 Simulation model diagram of heat dissipation

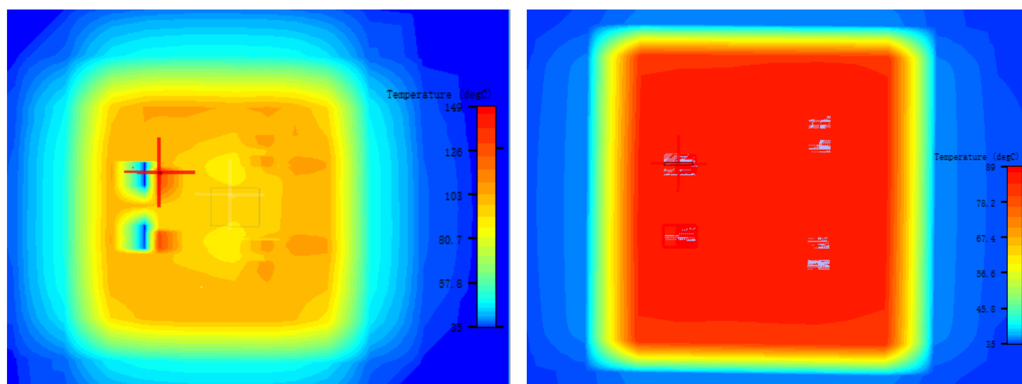

（a） Heat dissipation result with FR4 （b） Heat dissipation result with DBC（Al_2O_3）

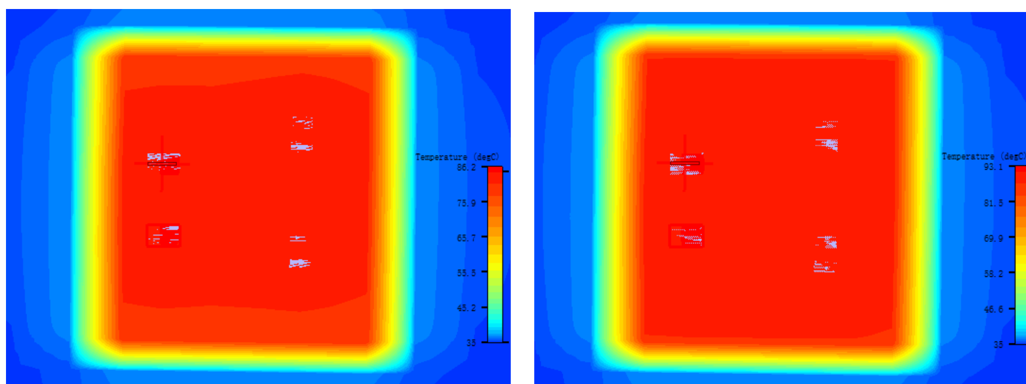

（c） Heat dissipation result with DBC（AlN） （d） Heat dissipation result after optimization

Figure 3-16 Simulation results of heat dissipation scheme

By analyzing the simulation results above, it is found that the heat dissipation of traditional FR4 is up to 149°C, which is not satisfied with the design requirements of the converter. The heat dissipation effect of the DBC scheme is the best, and the maximum temperature is 86.2

and 89°C. Respectively, while the optimized scheme result has little difference from the DBC heat dissipation, reaching 93.3°C.

This part mainly focuses on the structural layout of Gan devices. First, the advantages and disadvantages of several common structures are compared. Then the structural design of the optimized design is introduced. Finally, the FloTHERM is used to compare the traditional structure with the optimized structure, and the feasibility of the optimized structure design in the heat dissipation is determined.

3.5 Design of control and drive circuit

In this part, the design of the converter control drive circuit is discussed mainly. In order to avoid the influence between the digital control loop and the power loop, this design will isolate the various parts, and the structure is shown in Figure 3-17.

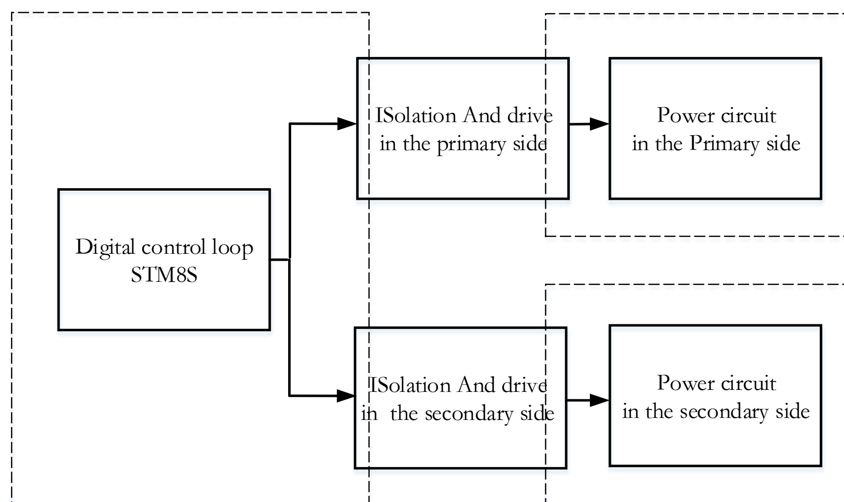

Figure 3-17 Diagram of control and drive circuit

3.5.1 Design of control circuit

In the control part of the converter, the commonly used control methods are digital control and analog control.

The analog control is based on the special power supply control chip. It has the advantages of small size, simple circuit design, low cost and so on. But at present, the frequency of the analog chip is usually from several hundred Hz to several thousand Hz. So the analog chips used in the high frequency field are relatively rare.

Digital control is mostly based on digital signal processor (DSP) or microprocessor (MCU). Compared with analog control, the biggest advantage of digital control lies in the realization of complex control algorithms and power management.

In this paper, the LLC resonant converter is designed to work near the resonant frequency to achieve maximum efficiency. The converter does not need sampling circuit and feedback control, and the working mode is simple. Comparing the advantages and disadvantages of the above analog control and digital control, the digital control method is adopted to design the control system. Because only the output of the control PWM waveform is realized, it is possible to choose a single chip with simple structure and small size as a digital control chip. Here the digital chip, STM8S003F3P6 produced by STMicroelectronics is chosen because of its simple structure, small size, good stability and so on.

STM8S's clock controller is powerful, flexible and easy to use. It has good performance and low power loss. The clock source of STM8S is divided into the internal clock source and the external clock source. The internal clock source is divided into 128kHz low speed oscillator and 16MHz high speed oscillator, and the external clock source can be connected with the external oscillator or clock signal of the 1~24MHz.

In this design, we mainly use the 16MHz high speed internal oscillator (HSI) as the main clock of the controller. Without external devices, the HSI can provide a low-cost 16MHz clock source with a duty cycle of 50%. We can control the dead time of output PWM waveform by changing register data. However, because HIS is the clock source of 16MHz, the minimum unit time is 62.5ns, and we can use the dead time of 62.5ns or 125ns in the actual design of the converter. The high speed internal oscillator starts faster than the high speed external oscillator. However, the accuracy is lower than that of high speed external crystal oscillator. The 1~24MHz high speed external oscillator can be used as the clock source in the design. This ensures that the dead time is flexible and adjustable, and the control accuracy can be improved. The only drawback is the need to add external oscillator, which may increase the volume of the converter.

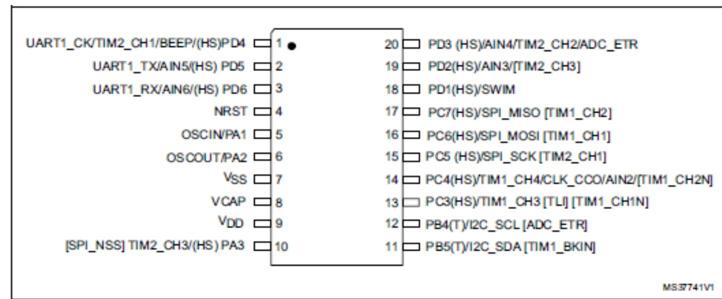

(a) Package schematic diagram (b)Pin diagram

Figure 3-18 Package and pin diagram of STM8S003F3P6

3.5.2 Selection and optimization of isolation and drive chip

The input voltage of the converter is 270V, and the output voltage is 28V. Because the input and output voltage difference is very large, the primary side should be designed different ground circuits for the safety of operation. And the high and low voltage levels should also be isolated, especially the switch tube drive isolation so that the driver works reliably. It can also avoid the influence of the large current to the digital signal and causing the switch tube to mislead. So this paper designs three separate isolation parts: the primary side power part, the secondary side power part and the digital control part, so that the isolation between the primary side, the secondary side and the digital circuit is realized.

The isolation drive in this design is the chip Si8271. Si8271 is a gate driver with longer service life and higher reliability produced by Silicon. Si8271 sets drive, isolation function in one, using 2.5~5.5 V digital power supply and 4.2~30 V analog power supply. It can isolate the 2.5kV voltage in a common package of 8 feet of the SOIC package. High integration, low transmission delay, smaller installation size, flexibility, and cost-effectiveness make Si8271 an ideal gate drive for various MOSFET, IGBT, SiC, and GaN FET. Compared with the combination of the isolating chip Si8610 and the driver chip LM5114, the Si8271 integrates the drive and isolation functions, which means that the design of the control drive circuit will be greatly simplified, using less drive isolation chips and external decoupling capacitors, voltage stable capacitors, voltage divider resistors, and power supply regulator chips. It not only saves cost, simplifies the debugging steps, but also greatly reduces the space and effectively improves the power density of the converter.

The switching speed of GaN devices can be controlled by gate resistance. Driving resistance from output to switch gate is critical to optimizing switching performance and driving

stability. Si8271 provides independent vo+ pins and vo- pins. As shown in Figure 5-3, we can separately design the turn-on gate resistor and the turn-off gate resistor to optimize the drive circuit, such as Figure 5-4. The turn-on gate resistor R_{GON} controls the voltage slew rate (dv/dt). When the turn-on gate resistor is too small, the gate voltage and the leakage current oscillate seriously, which will bring about greater switching loss and increase the risk of misleading, and the turn-on gate resistor will increase the opening time and also increase the loss. Usually GaN device manufacturers recommend resistance to 10~20Ω, which can also be determined according to actual engineering experiments. The turn-off gate resistor R_{GOFF} usually has a smaller value than R_{GON}, and the smaller the R_{GOFF}, the smaller the turn-off loss. But a too small R_{GOFF} may cause grid voltage oscillation, thereby increasing dead zone conduction losses or even misoperation. Usually, the GaN device manufacturer recommends a turn-off gate resistance of 1~3Ω.

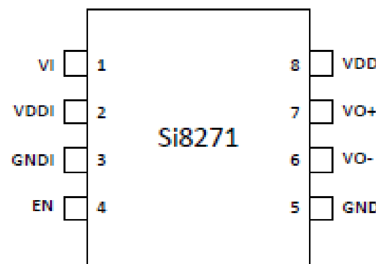

Figure 3-19 Pin diagram of Si8271

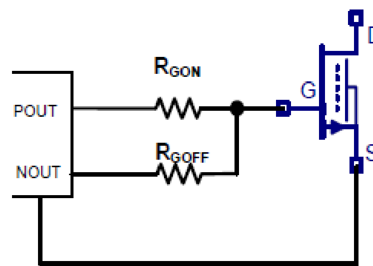

Figure 3-20 Diagram of driving resistance optimization

3.5.3 Layout optimization of PCB

In the first chapter, because of the cause of the junction capacitance of the Gan device, it is sensitive to the fast changing current in the branch. And the gate driven charge of the Gan device is very small, for example, the gate drive charge of GS66508T is only 5.8nC. So the device is also very sensitive to the parasitic inductance in the control loop. If the circuit is not designed properly, it may cause the overvoltage of the switch device, which will

eventually lead to the influence of EMI exceeding the standard, the misoperation of the circuit, the damage of the device and so on.

The absolute maximum rated voltage of the GS66508T gate is -10 ~ +7V. But when the gate voltage is between 4.5 ~6 V, the device can conduct well. So there is only about 1~2V voltage driving noise tolerance. In addition, the threshold voltage of GS66508T is only 1.3V. When the driving turns off, the oscillation phenomenon caused by parasitic inductance is created, so the switch tube is possible to be misled. The absolute maximum rated voltage of the secondary side switch EPC2032 gate is -4 ~ +6V. Only when the gate voltage is between 3.5 ~5 V, can the conduction effect be satisfied. Therefore, there is only about 1~2V voltage driving noise tolerance, and its threshold voltage is only 1.4V. In order to reduce the voltage oscillation in the driving circuit and avoid the breakdown of the device effectively, the parasitic inductance in the drive circuit should be minimized in the design process.

In this section, we optimize the wiring of the drive circuit and strictly control the parasitic inductance in the loop. Because the GaN switch device and other devices are arranged on both sides of the PCB board respectively, and the PWM wave produced by the control loop is 3.3V square wave, which is smaller than the input voltage 270V, when the converter power loop flows through the larger current or the higher voltage, the parasitic inductance in the loop will be produce common mode voltage. This leads to a high level at the isolated driven input port, which may eventually cause the switch tube misleading. Therefore, before the PWM wave enters the isolation drive chip, a small capacitor should be connected to counteract the common mode influence caused by the parasitic inductance.

The PCB wiring structure used in this design is shown in Figure 3-21.

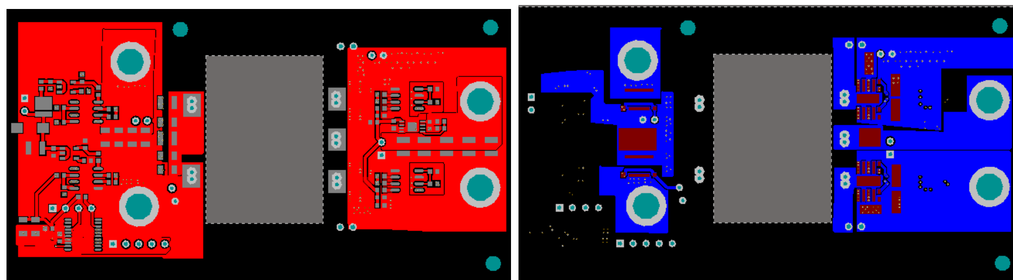

(a) Wiring on the top (b) Wiring on the bottom

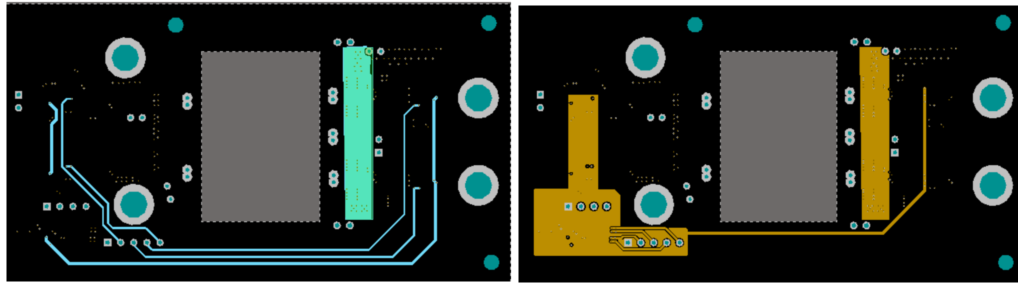

(c) Wiring on the signal 1 (d) Wiring on the signal 2

Figure 3-21 Diagram of PCB wiring

4 EXPERIMENT AND RESULT ANALYSIS

4.1 Experimental platform and prototype

This design sets up an experimental platform as shown in Figure 4-1. The name and function of the instrument are shown in Table 4-1.

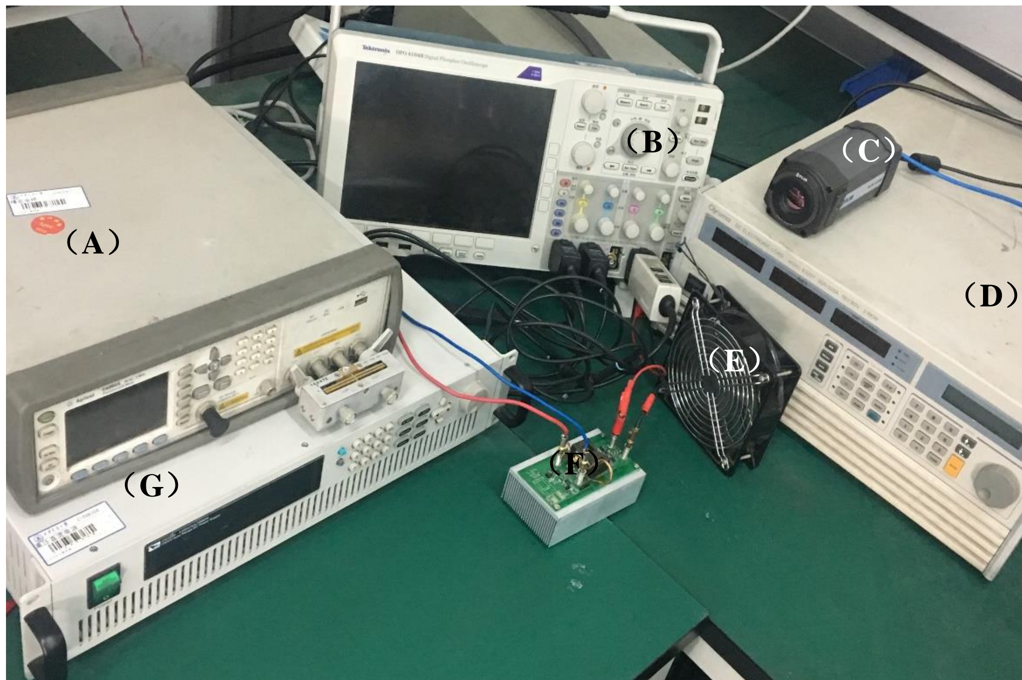

Figure 4-1 Platform for the experiment

Table 4-1 Name and function of the instrument

ID	Name	Model / Effect
（A）	LCR meter	E4980A
（B）	Oscilloscope	DPO4104B
（C）	Thermal imager	iM2300-C-00009
（D）	Programmable DC electronic load	Chroma 63201

(E)	Fan	Dissipate heat
(F)	Converter	Power module and heat dissipation
(G)	Programmable DC source	IT6726V

The experimental prototype is shown in Figure 4-2. The device selection and parameters of the prototype are shown in Table 4-2.

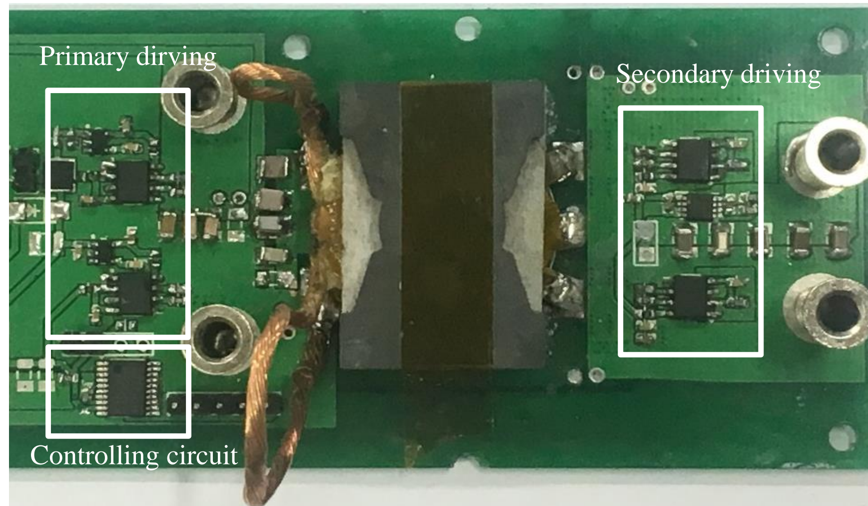

(a) Front of the converter

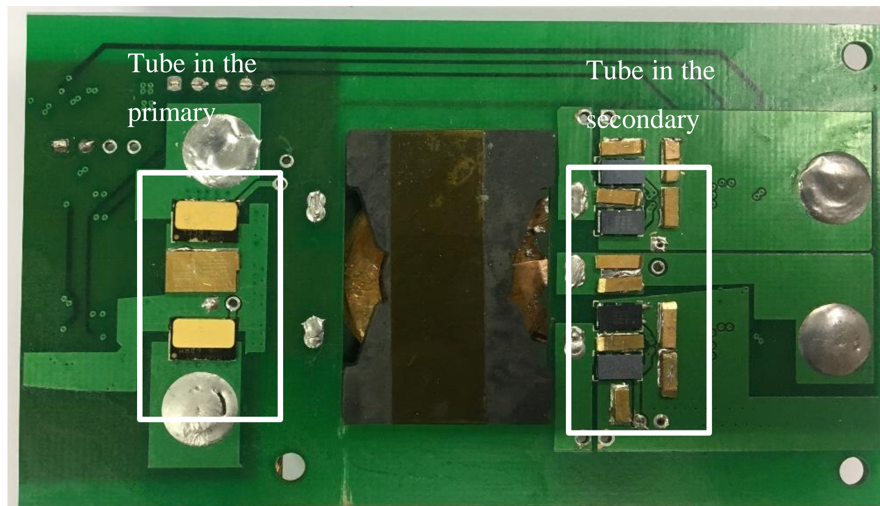

(b) Back of the converter

Figure 4-2 Prototype for the experiment

Table 4-2 Device selection and parameter of prototype

Device	Model Number
Switch tube in the primary	GS66508T

Synchronous rectifying tube	EPC2032
Isolating drive chip	Si8271
Magnetizing inductance / μH	17.2
Resonant inductor /nH	560
Resonant capacitor/nF	45

4.2 Experimental results and analysis

The output PWM waveform of the control loop of the LLC resonant converter is tested as shown in Figure 4-3. This is the digital part, so there is some oscillation and a certain time margin between the secondary side and the primary sid. Figure 6-4 is the drive circuit output signal, V_{gs_S1} and V_{gs_S2} are the primary side driving signal, and V_{gs_SR1} and V_{gs_SR2} are the secondary driving signal. By contrast, it can be found that after the isolation drive chip, the oscillation on the signal and the interference caused by each switch are significantly reduced. The secondary side drive signal still has a certain degree of oscillation when it is turned off. Because the threshold voltage of GaN is higher, it will not cause any impact. Because the primary side is the half bridge structure, the driving signal of the upper tube and the lower tube are not common. And there is also voltage isolation between the primary side and the secondary side, so the driving signals should be measured separately.

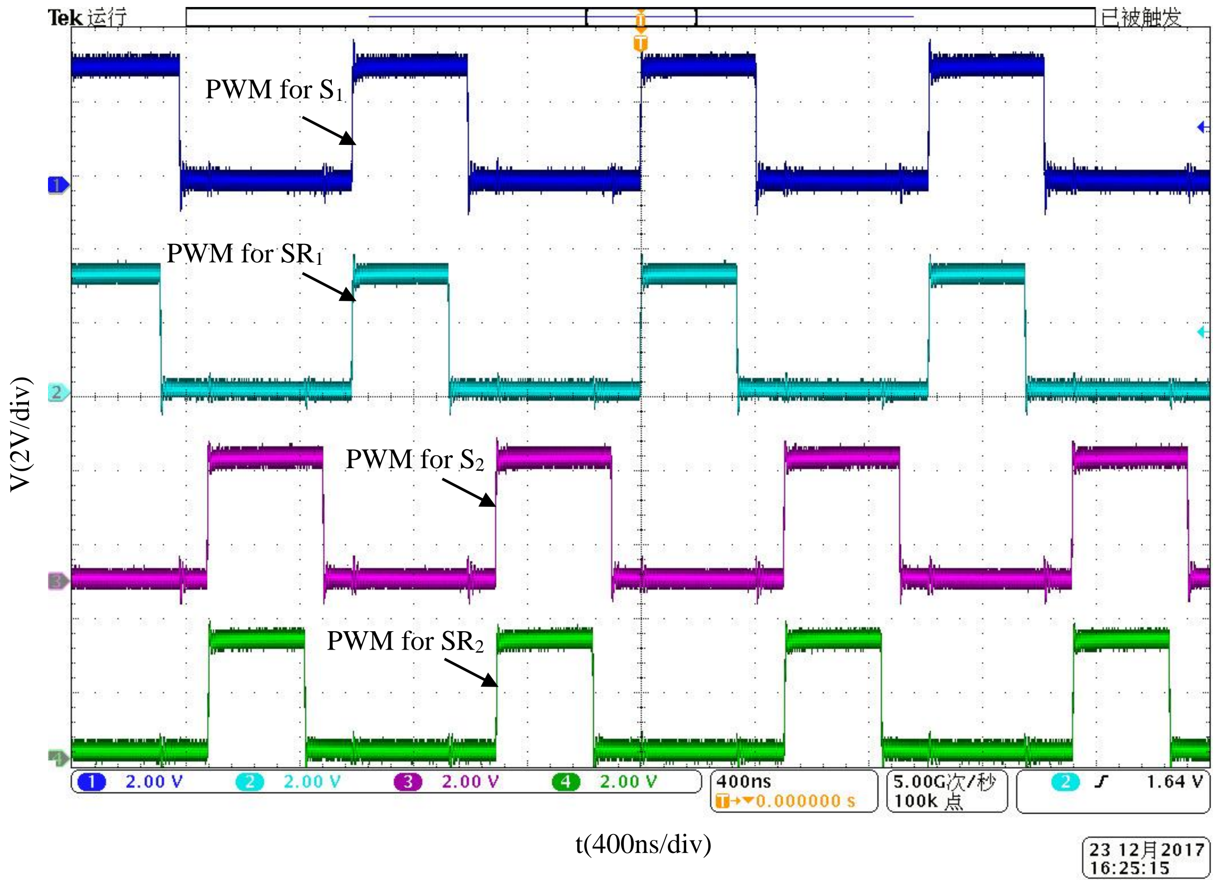

Figure 4-3 Waveform of PWM

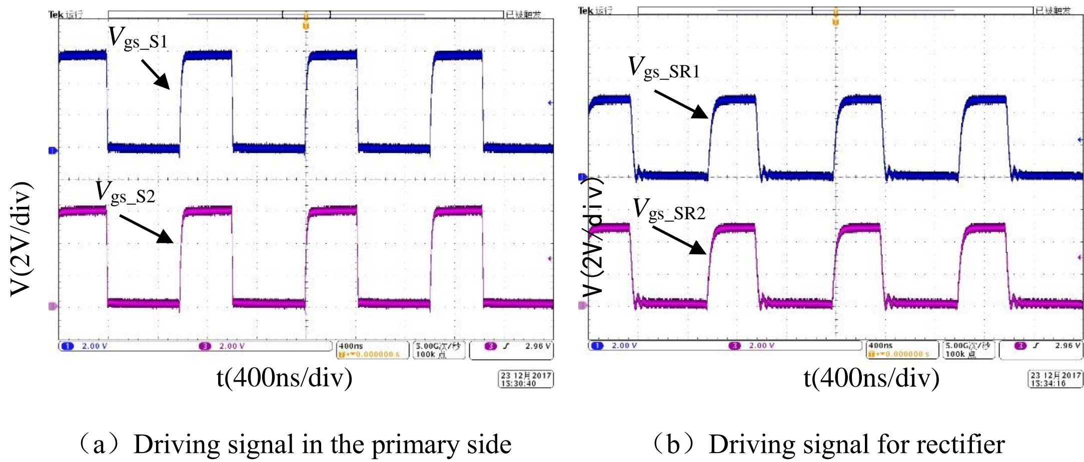

（a）Driving signal in the primary side （b）Driving signal for rectifier

Figure 4-4 Driving waveform

Measurement of the neutral point voltage V_m and the waveform of the lower tube drive signal V_{gs_S2} can be obtained as shown in Figure 4-5. It can be found that the neutral point potential is almost zero at the turn-on time of the lower tube, which can be considered as ZVS.

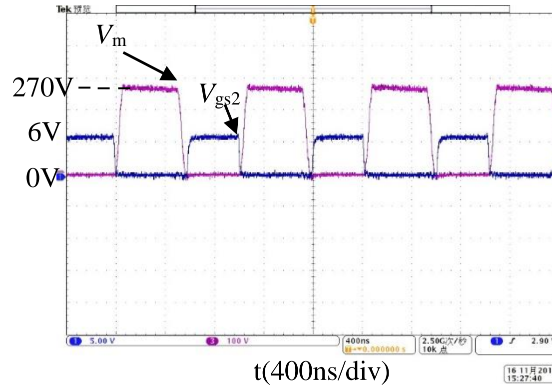

Figure 4-5 Waveform of V_m and V_{gs_S2}

The power circuit experimental waveforms are shown in Figure 4-6, the lower tube driving voltage waveform and the resonant current waveform in which (a), (b) and (c) are no-load, half load and full load. The resonant current I_r in the picture is approximately sinusoidal in the dead time, indicating that the converter works near the resonance point. In the dead time, the resonance current oscillates because of the oscillation of the transformer's secondary leakage and synchronous rectifier capacitance. Therefore, in the design of transformers, the leakage inductance of the two sides should be minimized.

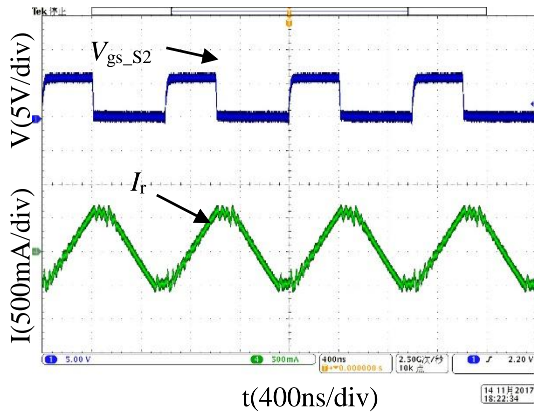

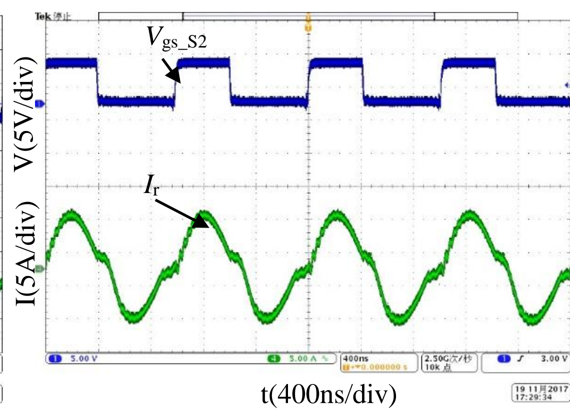

（a）No-load experimental waveform diagram　　（b）Half-load experimental waveform diagram

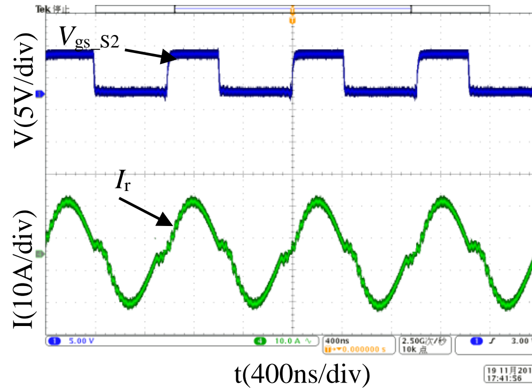

（c）Full-load experimental waveform diagram

Figure 4-6 Experimental waveform diagram

Figure 4-7 the temperature distribution image obtained by thermal imager during the operation. Because the power switch tubesare under the PCB board and are completely blocked by the radiator, the power tube temperature can not be measured directly. This is the defect of this design structure. The highest temperature in the picture is stable at around 44.6℃, which meets the design requirements. The highest temperature occurs on the secondary side synchronous rectifier driving power supply LDO. Because itconverted the output voltage of 28V to 5V drive voltage, the efficiency is very low. And its volume is small, so it is the most hot part to control the driving circuit.

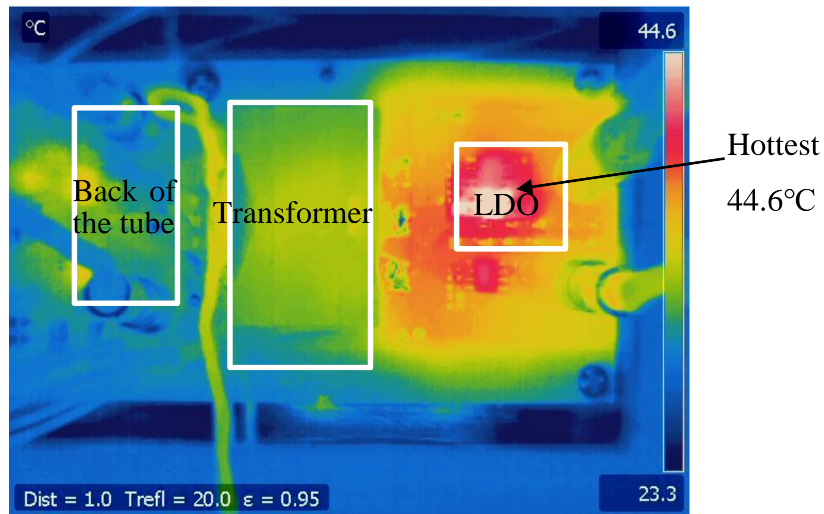

Figure 4-7 Temperature distribution diagram on the front of the converter

Finally, according to the prototype, the efficiency curve of the LLC resonant converter is shown in Figure 4-8. The efficiency of the prototype can be over 93.5%, and its maximum efficiency can reach 97.6%. The curve reaches the maximum efficiency around 200W. It

shows that after the output power is improved, the resistance loss and copper loss of each part of the design become the main part of the loss, and the final loss is larger than the calculated loss. The main reason is that the consumption of the power circuit of the PCB board is not included, and the loss of the transformer copper loss is not tested. Consider the effect of temperature on resistance, reducing the corresponding loss can be used as the main way to improve efficiency in future, such as selecting the thickness of copper layer of PCB board and reducing the length of wiring.

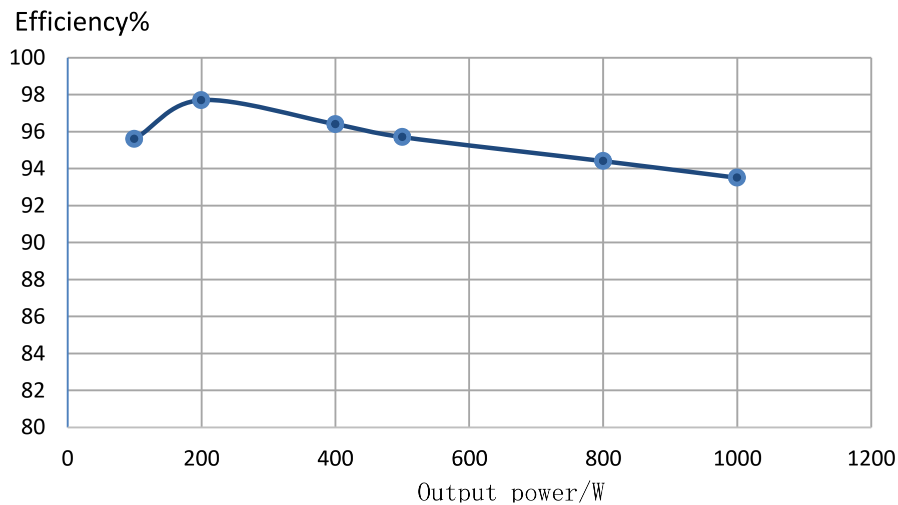

Figure 4-8 Experimental efficiency curve of prototype

4.3 Summary

In this chapter, a prototype of LLC resonant converter is designed and manufactured. The working principle is verified experimentally in the existing experimental platform, and the main experimental waveforms are given.

5 CONCLUSION AND PROSPECT

Due to its natural advantages and low conduction loss in high frequency applications, GaN devices have attracted widespread attention since its emergence. In recent years, the development of Si devices is close to the theoretical limit, but the demand for high efficiency and high power density power supply is still developing. The three generation of wide band gap semiconductor devices such as GaN devices has gradually become a hot topic in the power industry. With the continuous development of research, GaN devices are constantly improving in packaging design, stability of work, heat dissipation design and loss. This opens up vast space for its subsequent application. Compared with the PWM controlled topology converter, the LLC resonant converter has obvious advantages, especially the good performance of soft switching and stable control. The LLC resonant converter based on GaN sets the advantages of both of them, which makes the loss of the converter further reduced and the working frequency is further improved, which can effectively reduce the volume of the passive device and improve the power density of the converter. With planar transformer and synchronous rectification technology, it further meets the requirements of high efficiency and high power density converters.

In this paper, the working process and gain characteristics of LLC resonant converter are analyzed in detail. According to the demand, the selection of main components is introduced and the main parameters are calculated. The principle of LLC resonant converter is verified by LTspice software. Based on the heat dissipation problems of GaN devices, a comparison of the structural designs is carried out and a new structural design scheme is selected. All kinds of structural design schemes are simulated by FloTHERM thermal simulation software. The drive isolation device and the wiring structure of PCB are optimized. Finally, the input voltage 270V, the output voltage 28V, the LLC resonant converter operating at the 1MHz frequency, the full text design and optimization are finished, and the efficiency curve of the converter is obtained. Looking back on the whole process, we can get the following conclusions:

(1) The converter meets the design index: the input voltage is 270V, the output voltage is about 28V, the output power is 1kW, the efficiency of the whole machine is 93%~98%, and the power density is about 420 W/in^3.

(2) The LLC resonant converter can easily and simply realize the soft switching, effectively reducing the loss and improving the efficiency of the converter. In the parameter design of the LLC resonant network, the excitation inductor is very important. It not only involves the realization of the soft switcing, but also affects the efficiency of the converter. It should be carefully selected.

(3) The use of GaN devices can significantly improve the operating frequency of the converter, thus reducing the volume of transformers, inductors and capacitors. This will ultimately help to increase the power density of the converter. But the GaN device is more sensitive to the driving signal. In the design process, we should focus on the design of the driving wiring, try to reduce the parasitic inductance in the loop, make the driving signal not disturbed by the power loop, so as to ensure the normal work of the GaN device.

(4) The synchronous rectification of GaN device is less than that of conventional diode rectifier. When used with LLC resonant network, the timing and timing of synchronous switch are very important.

(5) When the GaN device is used in high power, the heat dissipation should also be considered. The optimized heat dissipation structure used in this paper can effectively reduce the thermal resistance of GaN devices to the air, which is beneficial to heat dissipation and to maintain the normal working temperature of the GaN devices.

In this paper, the above conclusions are obtained through theoretical research and simulation experiment, and the results have been achieved. However, in the process of research, we find that there are still a lot of content to be optimized.

The reverse conduction of partial GaN devices in synchronous rectification will cause large reverse losses. In this design, the synchronous rectification control mode of LLC resonant converter is relatively simple. In the future, the timing of synchronous rectification part can be further optimized to ensure normal operation of synchronous rectification while minimizing rectifier losses.

It is believed that by further optimization, the LLC resonant converter based on GaN devices can play a more excellent performance and play a greater role in the industrial power supply field.

6 REFERENCES

[1] Pei Yunqing, Yang Xu, Wang Zhaoan, "switching power supply design and application [M]. mechanical industry press. "2010.

[2] Deng ZY, "Research of Electromagnetic Compatibility Problem in Designing of High Frequency Switching-Mode Power Supply[J]," World of Power Supply, 2005, (06):69-75.

[3] Ren YC, Xu M, Sun JL and Lee FC, "A family of high power density unregulated bus converter[J] ," IEEE Transactions on Power Electronics, 2005, 20(5): 1045–1054.

[4] Ruan Xin Bo, Yan Yangon, "soft switching technology of pulse width modulation DC/DC full bridge converter [M]," Science Press, 1999.

[5] Zhao L, Li H, Hou Y, *et al.,* "Operation analysis of a phase-shifted full-bridge converter during the dead-time interval[J], " Iet Power Electronics, 2016, 9(9):1777-1783.

[6] Rudolf,P． Severns,"Topologies for Three-Element Resonant Converter[J]," IEEE Trans． On P． E． ,1992,7(1)：89—98．

[7] "Power Supply Design Seminar. Designing an LLC Resonant Half-Bridge Power Converter[OL]. [2010-01]. http://power.ti.com/seminars. " 2010.

[8] Steigerwald RL, "A comparison of half-bridge resonant converter topologies[J]. " IEEE Transactions on Power Electronics, 2002, 3(2):174-182.

[9] Yang B, "Topology investigation for front end dc/dc power conversion for distributed power system [D]. " Virgina Polytechnic Institute and State University, 2003.

[10] Cho SH, Kim CS, Han SK, "High-Efficiency and Low-Cost Tightly Regulated Dual-Output LLC Resonant Converter[J]. " IEEE Transactions on Industrial Electronics, 2012, 59 (7): 2982-2991.

[11] Yang B, Lee FC, Zhang AJ, *et al.,* "LLC resonant converter for front end DC/DC conversion[C]. " Applied Power Electronics Conference and Exposition (APEC).2002:1108-1112.

[12] Chen S, LüZ, Yao W, "Research and verification on LLC resonant soft switching DC-DC transformer[J]. " Transactions of China Electrotechnical Society, 2012, 27(10):163-169.

[13] Yang B, "Topology investigation for front end dc/dc power conversion for distributed power system [D], " Virgina Polytechnic Institute and State University, 2003.

[14] Y Fang, D Xu, Y Zhang, *et al.,* "Design of High Power Density LLC Resonant Converter with Extra Wide Input Range[C], " Applied Power Electronics Conference, APEC 2007 . 2007: 976 – 981.

[15] Zhu Lihong, Xu Dehong, "LLC resonant converter design [D]." Hangzhou: Zhejiang University,2006.

[16] Ren R, Liu S, Wang J, *et al.,* "High frequency LLC DC-transformer based on GaN devices and the dead time optimization[C]. " Electronics and Application Conference and Exposition. IEEE, 2014:462-467.

[17] Pearson GL, Brattain WH, "History of Semiconductor Research[J]. " Proceedings of the IRE, 1955, 43 (12): 1794-1806.

[18] Wallich P. U.S, "semiconductor industry getting it together: Despite their history of intense competition, U.S. manufacturers are cooperating in research to gain an edge in the international marketplace[J]. " IEEE Spectrum, 1986, 23 (4): 75-78.

[19] Liang Chunguang, Zhang Ji, "GaN - third generation semiconductor dawn [J]." semiconductor Journal,1999：20 (2)：89－89.

[20] Lidow A, Johan S, Rooij MD, *et al.,* "GaN transistors for efficient power conversion : the eGaN FET journey continues[M]. " Power Conversion Publications, 2011.

[21] Wang Dandan, "theoretical research on wide band gap semiconductor photoelectric functional materials" [D]., Chinese Academy of Sciences,2015.

[22] Wang KP, Yang X, Ma H, *et al.,* "An Analytical Switching Process Model of Low-Voltage eGaN HEMTs for Loss Calculation[J]. " Power Electronics, IEEE Transactions on, 2015,PP(99): 1-1.

[23] Wang KP, " An optimized layout with split bus capacitors in eGaN-based integrated DC-DC converter module[C]. " Ma H,Yang X. 2014 International Power Electronics and Application Conference and Exposition (PEAC2014), 2014.

[24] Wang KP, "An Optimized PCB Layout with Low Parasitic Inductances for Gallium Nitride Based DC-DC Converter[C]. " Ma H, Li HC. Applied Power Electronics Conference and Exposition (APEC). 2015.To be published.

[25] Zhang W, Wang F, Costinett D, *et al.,* "Investigation of Gallium Nitride Devices in High Frequency LLC Resonant Converter[J]. " IEEE Transactions on Power Electronics, 2016:1-1.

[26] Hughes B, Lazar J, Hulsey S, *et al.,* "Analyzing losses using junction temperature of 300V 2.4kW 96% efficient, 1MHz GaN synchronous boost converter[C], " 2013: 131-134.

[27] Yamamoto N, Hiraki E, Tanaka T, *et al.,* "A study on GaN inverter based MHz frequency induction heating for tiny metals[C], " 2013: 5023-5027.

[28] Čučak D, Vasić M, Garc ía O, *et al.,* "Optimum design of an envelope tracking buck converter for RFPA using GaN HEMTs[C], "2011: 1210-1216.

[29] Wang K, Yang X, Ma H, *et al.,* "An Analytical Switching Process Model of Low-Voltage eGaN HEMTs forLoss Calculation[J]. " Power Electronics, IEEE Transactions on, 2015,PP(99): 1-1.

[30] Danilovic M, "Evaluation of the switching characteristics of a gallium-nitride transistor[C]. " Chen Z, Wang R, *et al.,* Energy Conversion Congress and Exposition (ECCE), 2011: 2681-2688.

[31] Erickson, "Fundamentals of Power Electronics[M]. " Fundamentals of power electronics. CRC Press , 2000

[32] Chen Guohua, "soft ferrite materials and components development trends twenty-first Century" [J]. magnetic materials and devices.2001, 32 (4):34-36.

[33] Li J, Shi Y, Niu Z, *et al.,* "Modeling, simulation and optimization design of PCB planar transformer[C]. " Eighth International Conference on Electrical Machines and Systems. IEEE, 2005:1736-1739 Vol. 3.

[34] Dai N, Lofti AW, Skutt G, *et al.,* "A comparative study of high-frequency, low-profile planar transformer technologies[C]. " IEEE APEC, Orlando, USA, 1994: 226-232.

[35] Vijaya Kumar N, Satpathy S, Lakshminarasamma N, "Analysis and design methodology for Planar Transformer with low self-capacitance used in high voltage flyback charging circuit[C], " 2016: 1-5.

[36] Ho GKY, Fang Y, Pong BMH, *et al.,* "Printed circuit board planar current transformer for GaN active diode[C], " 2017: 2549-2553.

[37] D. Huang, S. Ji, and F. C. Lee, "LLC resonant converter with matrix transformer[J]. " IEEE Trans. on Power Electron., vol. 29, no. 8, pp.4339-4347, Aug. 2014.

[38] M. Mu and F. C. Lee, "Design and Optimization of a 380V-12V High-Frequency, High-Current LLC Converter with GaN Devices and Planar Matrix Transformers[J]. " IEEE Journal of Emerging and Selected Topics in Power Electronics, vol. 4, no. 3, pp. 854-862, Sep. 2016.

[39] Fei C, Lee FC, Li Q, "High-efficiency high-power-density 380V/12V DC/DC converter with a novel matrix transformer[C], " 2017: 2428-2435.

[40] Yan R, Tang S, Xi J, *et al.,* "A GaN HEMTs half-bridge driver with bandgap reference comparator clamping for high-frequency DC-DC converter[C], " 2017: 539-545.

[41] Gu L, Liang W, Davila JR, "Design of very-high-frequency synchronous resonant DC-DC converter for variable load operation[C], " 2017: 3447-3454.

[42] Ramachandran R, Nymand M, "Switching losses in a 1.7 kW GaN based full-bridge DC-DC converter with synchronous rectification[C], " 2015: 1-10.

[43] Fu D, Lu B, Lee FC. "1MHz High Efficiency LLC Resonant Converters with Synchronous Rectifier[C], " 2007: 2404-2410.

[44] Hsieh GC, Tsai CY, Hsu WL, "Synchronous Rectification LLC Series-Resonant Converter[C], " 2007: 1003-1009.

[45] Mohammadi M, Shafiei N, Ordonez M. "LLC synchronous rectification using Coordinate Modulation[C], " 2016: 848-853.

[46] Mohammadi M, Ordonez M. "LLC synchronous rectification using homopolarity cycle modulation[C], " 2017: 3776-3780.

[47] Fei C, Lee FC, Li Q, "Digital implementation of adaptive synchronous rectifier (SR) driving scheme for LLC resonant converters[C], " 2016: 322-328.

[48] Iorio A, Bianco A, Foresta M, *et al.,* "Predictive adaptive method for synchronous rectification[C], " 2015: 1986-1992.

[49] Tan Linlin, "research and design of 500W LLC resonant converters using GaN devices" [D], Xi'an Jiao Tong University.2017.